Cell

Beclin1 Controls the Levels of p53 by Regulating the Deubiquitination Activity of USP10 and USP13

Junli Liu,[1,5] Hongguang Xia,[1,5] Minsu Kim,[2,6] Lihua Xu,[1,6] Ying Li,[1,2,6] Lihong Zhang,[1,6] Yu Cai,[1] Helin Vakifahmetoglu Norberg,[2] Tao Zhang,[1] Tsuyoshi Furuya,[2] Minzhi Jin,[1] Zhimin Zhu,[2] Huanchen Wang,[3] Jia Yu,[1] Yanxia Li,[1] Yan Hao,[1] Augustine Choi,[4] Hengming Ke,[3] Dawei Ma,[1,*] and Junying Yuan[2,*]

[1]State Key Laboratory of Bioorganic and Natural Products Chemistry, Shanghai Institute of Organic Chemistry, Chinese Academy of Sciences, 354 Fenglin Lu, Shanghai 200032, China

[2]Department of Cell Biology, Harvard Medical School, 240 Longwood Avenue Boston, MA 02115, USA

[3]Department of Biophysics and Biochemistry, University of North Carolina at Chapel Hill, Chapel Hill, NC 27599, USA

[4]Brigham and Women's Hospital, 75 Francis Street, Boston, MA, 02115, USA

[5]These authors contributed equally to this work

[6]These authors contributed equally to this work

*Correspondence: madw@mail.sioc.ac.cn (D.M.), jyuan@hms.harvard.edu (J.Y.)

DOI 10.1016/j.cell.2011.08.037

SUMMARY

Autophagy is an important intracellular catabolic mechanism that mediates the degradation of cytoplasmic proteins and organelles. We report a potent small molecule inhibitor of autophagy named "spautin-1" for *s*pecific and *p*otent *aut*ophagy *in*hibitor-*1*. Spautin-1 promotes the degradation of Vps34 PI3 kinase complexes by inhibiting two ubiquitin-specific peptidases, USP10 and USP13, that target the Beclin1 subunit of Vps34 complexes. *Beclin1* is a tumor suppressor and frequently monoallelically lost in human cancers. Interestingly, Beclin1 also controls the protein stabilities of USP10 and USP13 by regulating their deubiquitinating activities. Since USP10 mediates the deubiquitination of p53, regulating deubiquitination activity of USP10 and USP13 by Beclin1 provides a mechanism for Beclin1 to control the levels of p53. Our study provides a molecular mechanism involving protein deubiquitination that connects two important tumor suppressors, p53 and Beclin1, and a potent small molecule inhibitor of autophagy as a possible lead compound for developing anticancer drugs.

INTRODUCTION

Vps34 is the primordial member of the PI3 kinase family and the only known class III PI3 kinase that can phosphorylate the D-3 position on the inositol ring of phosphatidylinositol (PtdIns) to produce PtdIns3P (Schu et al., 1993). In contrast to class I PI3 kinase, which has been extensively studied, much less is known about the class III PI3 kinase or its regulation in mammalian cells. Emerging evidence indicates a central role of Vps34 PI3K activity and its protein partners in orchestrating both initiation and maturation of autophagosomes (Simonsen and Tooze, 2009). Thus, exploring the mechanisms that regulate the class III PI3 kinase has direct implications in our understanding of these important intracellular mechanisms as well as for developing therapies for treatment of human diseases.

Similar to their homologs in yeast, Vps34 in mammalian cells is present in two complexes: Vps34 complex I and Vps34 complex II (Itakura et al., 2008; Liang et al., 2006; Matsunaga et al., 2009; Zhong et al., 2009). These two complexes share the core components of Vps34, Beclin1 and p150; and in addition, complex I contains Atg14L and complex II contains UVRAG. Interestingly, the stabilities of different components of Vps34 complexes are codependent upon each other as knockdown of one component often reduces the levels of others in the complexes (Itakura et al., 2008).

Beclin1 has been characterized as a tumor suppressor, and its importance is underscored by both the frequent monoallelic loss of *beclin1* in human breast, ovarian and prostate tumors, and an increased rate of malignant tumors in *BECN1*+/− mice (Liang et al., 1999; Qu et al., 2003; Yue et al., 2003). Although autophagy deficiency has been proposed to be the mechanism for the increased tumorigenesis in *BECN1*+/− mice, a recent study using tissue-specific knockout mice of Atg5 and Atg7 suggests that autophagy deficiency may lead to benign tumors in livers, but not in other tissues (Takamura et al., 2011). Thus, the mechanism of Beclin1 as a tumor suppressor remains as a puzzle.

Small molecule inhibitors are important tools in exploring the cellular mechanisms in mammalian cells. However, the only available small molecule inhibitor of autophagy is 3-methyladenine (3-MA), which has a working concentration of ~10 mM and inhibits multiple forms of PI3 kinases. Therefore, there is an urgent need to develop highly specific small molecule tools that can be used to facilitate the studies of autophagy in mammalian cells. Using an imaging-based screen, we identified a small molecule inhibitor of autophagy and developed it into a highly potent autophagy inhibitor. We named it "spautin-1" for *s*pecific and *p*otent *aut*ophagy *in*hibitor-1. We explored the

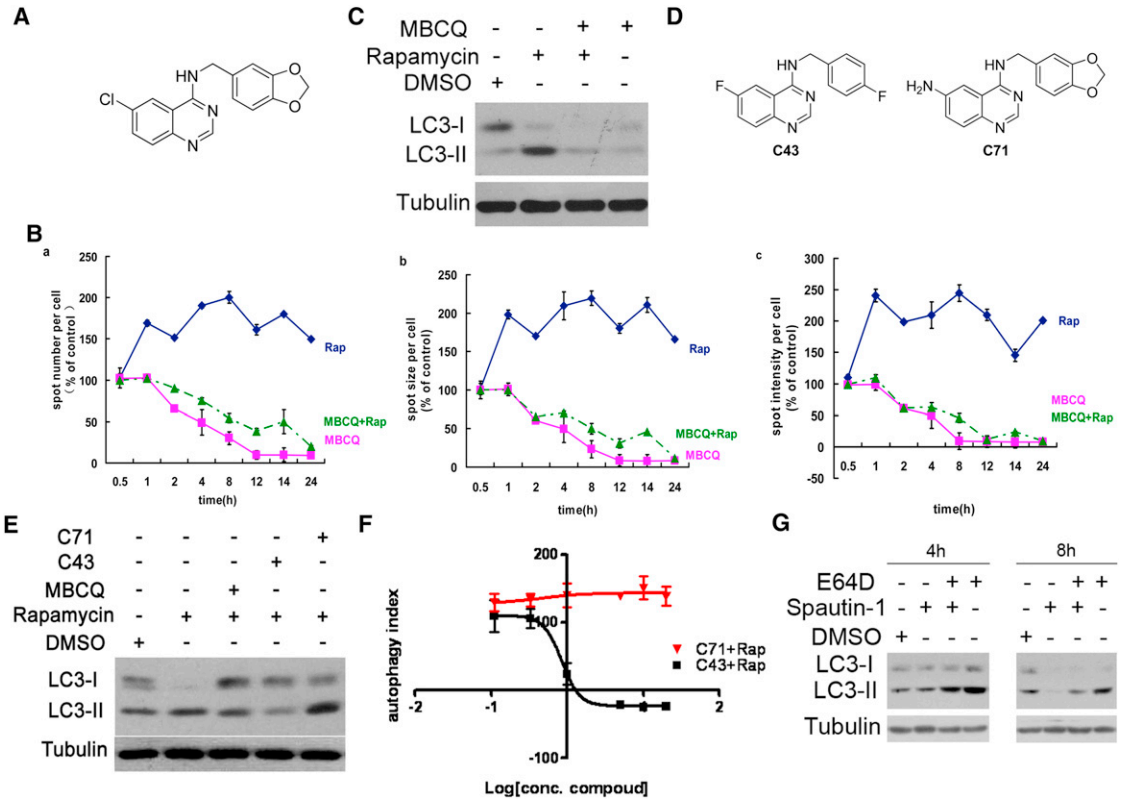

Figure 1. Isolation of a Series of Small Molecule Inhibitors of Autophagy

(A) The structure of MBCQ.

(B) MBCQ reduced the spot numbers (a), spot size (b), and spot intensity (c) of LC3-GFP$^+$ puncta. H4-LC3-GFP cells were treated with rapamycin (0.2 μM) and MBCQ (5 μM) as indicated. The image data are expressed as % of control vehicle treated cells. 1000 cells were analyzed per treatment condition.

(C) H4-LC3-GFP cells were treated with rapamycin (0.2 μM) and MBCQ (10 μM) as indicated for 2 hr and the cell lysates were analyzed by western blotting using anti-LC3. β-tubulin was used as a control.

(D) An active (C43=spautin-1) and an inactive (C71) derivatives of MBCQ.

(E) MEF cells were treated with DMSO (1‰), rapamycin (0.2 μM) alone, or together with MBCQ (10 μM), C43 (10 μM) or C71 (10 μM) for 4 hr. The cell lysates were analyzed for western blotting using anti-LC3 antibody. β-tubulin was used as a loading control.

(F) Dose-response (in μM) of C43 and inactive C71. H4-LC3-GFP cells were treated with rapamycin (0.2 μM) for 12 hr with C43 or C71 as indicated. The LC3-GFP$^+$ puncta were quantified as in (B). Autophagy index = % {[total LC3-GFP$^+$ spot intensity (compound+rapamycin treated) per cell] – [total LC3-GFP$^+$ spot intensity (DMSO treated) per cell]} / {[total LC3-GFP$^+$ spot intensity (rapamycin treated) per cell] – [total LC3-GFP$^+$ spot intensity (DMSO treated) per cell]}. Rap = rapamycin.

(G) H4-LC3-GFP cells were treated with spautin-1(10 μM) with or without E64D (5 μM) for indicated periods of time. The cell lysates were analyzed by western blotting using anti-LC3 and anti-β-tubulin.

All error bars indicate STD. See also Figure S1 and S2.

mechanism by which spautin-1 inhibits autophagy and found that it inhibits two ubiquitin specific peptidases, USP10 and USP13, which regulate the deubiquitination of Beclin1 in Vps34 complexes. Using spautin-1 as a tool, we explored the interaction of USP10 and USP13 with Vps34 complexes. Interestingly, we found that Vps34 complexes interact with USP13 and the stabilities of USP10 and USP13 are coordinately regulated with that of Vps34 complexes. Since USP10 is a deubiquitinating enzyme for p53 and regulates the levels of p53 by controlling p53 ubiquitination and degradation (Yuan et al., 2010), regulating the stability of USP10 and USP13 by Vps34 complexes provides a molecular mechanism for class III PI3 kinase to control the levels of p53. Indeed, as predicted by our model, we found that the levels of p53 are reduced in the tissues of *BECN1*+/− mice, which provide a molecular mechanism for the increased tumorigenesis after monoallelic loss of *beclin1*. Our results demonstrate that class III PI3 kinase is an important tumor suppressor that can regulate the levels of p53 through controlling its deubiquitination.

RESULTS

Isolation of a Small Molecule Inhibitor of Autophagy by an Image-Based Screen

In an imaging-based screen using LC3-GFP as a marker for autophagy (Zhang et al., 2007), we identified a small molecule inhibitor of autophagy, MBCQ, from the ICCB known bioactive library (Figure 1A). MBCQ was previously known as an inhibitor

of phosphodiesterase type 5 (PDE5), an enzyme that degrades cGMP by hydrolysis (MacPherson et al., 2006). Stimulation of H4-LC3-GFP cells with rapamycin led to increases in the levels of LC3-GFP as expected. A quantitative analysis of LC3-GFP puncta using high throughput microscopy showed that the treatment of MBCQ reduced the spot numbers as well as spot size and spot intensity of LC3-GFP dots compared to that of control or rapamycin treatment alone (Figure 1B). Thus, the presence of MBCQ inhibited both basal as well as rapamycin induced LC3-GFP autophagic puncta.

This result was further confirmed by LC3 western blot analysis (Figure 1C), and similar results were obtained using mouse embryonic fibroblast cells (MEFs) (Figure S1A). Inhibition of autophagy by MBCQ was rapid (Figure 1B) and dose-dependent with an IC_{50} of 0.8 μM (Figure S1B), which is significantly more potent than the commonly used class III PI3 kinase inhibitor, 3-methyladenine (3-MA). We have also confirmed the autophagy inhibitory activity of MBCQ by electron microscopic studies. Cells treated with rapamycin showed a large number of autophagosomes with characteristic double membrane, which were conspicuously absent in cells treated with rapamycin and MBCQ (Figure S1C). Finally, the treatment of MBCQ was able to reduce the autophagic puncta of LC3-GFP in the presence of rapamycin, under starvation conditions or with bafilomycin which blocks lysosomal degradation (Figure S1D). Thus, MBCQ is an upstream inhibitor of autophagy.

Autophagy-Inhibiting Activity of MBCQ Can Be Separated from Its PDE5-Inhibiting Activity

One hundred and twelve derivatives of MBCQ were synthesized and analyzed to determine if its activity in inhibiting autophagy could be separated from its inhibition of PDE5 (Table S1 and data not shown). The chemical synthetic schemes are shown in the Extended Experimental Procedures. We selected 9 MBCQ derivatives based on their efficacy in inhibiting autophagy and screened for their activities on PDE5 (Wang et al., 2008). We found that C43 (6-fluoro-N-[4-fluorobenzyl]quinazolin-4-amine), an effective autophagy inhibitor with an IC_{50} of 0.74 μM (Figure 1D-F), which is comparable to that of MBCQ, has significantly reduced activity toward PDE5 and other PDEs (Figures S2A and S2B and Table S1). Thus, the PDE5 inhibiting activity of MBCQ can be chemically separated from its autophagy inhibiting activity.

Consistent with a separation of PDE5 and autophagy inhibiting activities in MBCQ, there were a number of other known PDE5 inhibitors in the bioactive library that we screened, including MY-5445, dipyridamole, IBMX and sildenafil (Viagra), which were not identified as autophagy inhibitors. To further confirm this conclusion, we treated H4-LC3-GFP cells with rapamycin and other PDE5 inhibitors including MY-5445, dipyridamole, IBMX or sildenafil using MBCQ as a positive control. None of the specific PDE5 inhibitors tested, including the most potent PDE5 inhibitor, sildenafil (Viagra) which has an IC_{50} of 2.5 nM for PDE5, had any activity on autophagy (data not shown). Thus, we conclude that the autophagy inhibiting activity of MBCQ is not related to its PDE5 inhibiting activity.

To further examine the specificity of C43 in inhibiting autophagy, we treated mouse embryo fibroblasts (MEF) cells with C43 or C71, a negative control, in the presence of rapamycin with the levels of autophagy determined by LC3 western blotting. Treatment with C43, but not a negative control C71, inhibited autophagy induced by rapamycin (Figures 1D–1F) and starvation (Figure S2C). We also confirmed the inhibition of autophagy by C43 using electron microscopy (Figure S2D). Furthermore, the treatment of C43 inhibited autophagy activated in the presence of E64D, a protease inhibitor that increases the accumulation of autophagosome by blocking lysosomal degradation (Figure 1G). Based on these data, we conclude that C43 is a potent inhibitor of autophagy and named it "spautin-1" for specific and *p*otent *aut*ophagy *in*hibitor-1.

Spautin-1 Promotes Cell Death under Starvation Condition and Inhibits Autophagic Cell Death

We first characterized the biological effects of spautin-1 at the cellular level in a selected subset of cancer cell lines. Spautin-1 had no effect on the growth and survival of Bcap-37 cells under normal culture conditions (Figure 2A) but dramatically enhanced cell death in glucose-free media (Figure 2B). Bcap-37 cells treated with spautin-1 under glucose-free condition showed apoptotic morphology (Figure 2C) and characteristic PARP cleavage (Figure 2D). Western blotting for LC3 further confirmed that autophagy was induced under glucose-free conditions, which was inhibited by spautin-1 (Figure 2E). Similar results were obtained with MCF-7 and BT549 cells (data not shown). Thus, spautin-1 can sensitize tumor cells to apoptosis under nutritional deprived conditions.

In contrast to the above cancer cell lines analyzed, MDCK cells, a normal cell line derived from the Madin-Darby canine kidney, treatment with spautin-1 under glucose-free conditions did not undergo apoptosis (Figures S3A and S3B). Hs578Bst cells, a myoepithelial cell line established from normal tissue peripheral to a breast cancer, were also not sensitive to the treatment of spautin-1 (Figures S3C and S3D). These results are consistent with the proposal that cancer cells are under increased metabolic pressure and therefore more sensitive to inhibition of autophagy than that of normal cells (Karantza-Wadsworth et al., 2007).

Increased activation of autophagy in apoptosis deficient cells has been shown to mediate cell death (Shimizu et al., 2004). To test this possibility, we treated Bax/Bak double knockout (DKO) cells with etoposide to induce cell death by DNA damage in the presence or absence of spautin-1. We found that spautin-1 inhibited etoposide induced autophagic cell death of Bax-Bak DKO cells (Figures S3E–S3G). Thus, spautin-1 can be used as a tool to explore the requirement of autophagy in cellular processes.

Spautin-1 Selectively Promotes the Degradation of Vps34 Complexes

To explore the mechanism by which spautin-1 inhibits autophagy, we first examined the effects of spautin-1 on FYVE-RFP, an indicator for the activity of class III PI3 kinase, because PtdIns3P, the product of class III PI3 kinase, is important for the formation of autophagosomes (Gaullier et al., 1998; Simonsen and Tooze, 2009). Treatment with spautin-1 (Figure 3A) and MBCQ (Figure S4A) reduced the levels of FYVE-RFP puncta,

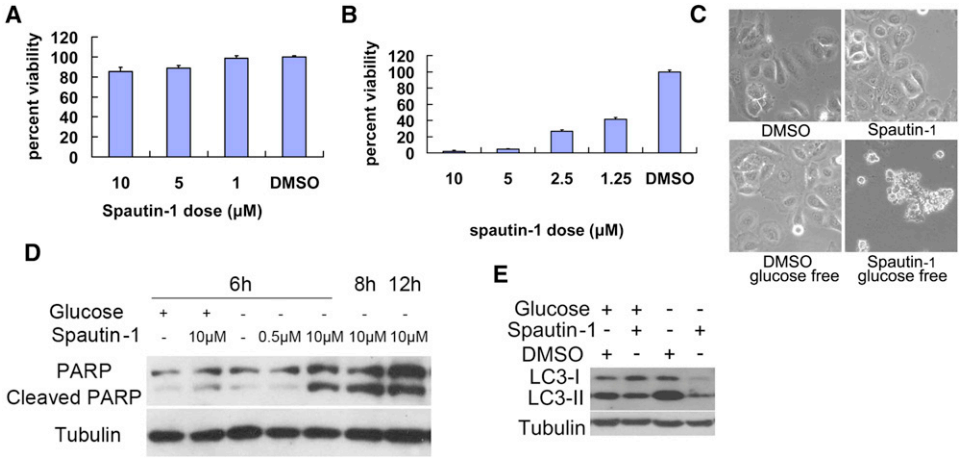

Figure 2. The Biological Effects of Spautin-1 on Cellular Models of Cell Death

Bcap-37 cells were treated with indicated compounds in normal DMEM with 10% bovine serum (A), glucose free condition (B) or both (C-E) for 48 hr. The cell viability was determined by MTT assay (A), (B), imaged using a phase contrast microscope (C) or the cell lysates were analyzed by western blotting using anti-PARP (D), anti-LC3 and anti-β-tubulin (as a control) (E). All error bars indicate STD. See also Figure S3.

but had no effect on the protein levels of FYVE-RFP (Figure S4B), suggesting that spautin-1 reduced the levels of PtdIns3P. The reduction of PtdIns3P in spautin-1 treated cells was confirmed using lipid dot blot analysis (Gozani et al., 2003)(Figure 3B). However, spautin-1 does not inhibit the lipid kinase activity of Vps34 in vitro (data not shown). Thus, spautin-1 can reduce the levels of PtdIns3P in cells, but is not a direct inhibitor of class III PI3 kinase activity.

Interestingly, we noted that the levels of Flag-Beclin1 and HA-Vps34 were considerably lower in spautin-1 treated cells than that of control cells (Figure 3C). In addition, treatment with spautin-1 also reduced the levels of GFP-p150 and Myc-Atg14L (Figures 3D and 3E). On the other hand, the treatment of spautin-1 had no effect on the protein levels of GFP alone, GFP-Arf1, GFP-MT, EGFR, HA-Hrs, HA-Atg3, or GFP-Atg7 (data not shown). Thus, spautin-1 selectively reduces the levels of exogenously expressed components of Vps34 complexes.

To determine if spautin-1 has a similar effect on endogenous Vps34 complexes, we conducted a time course study of H4-LC3-GFP cells treated with spautin-1 by western blotting. We found that the levels of endogenous Beclin1, Vps34, p150, Atg14L, and UVRAG progressively decreased in a time-dependent manner in the presence of spautin-1, and the effect of spautin-1 on the levels of Vps34 complexes was strongly correlated with that of LC3II (Figure 3F). Other active derivatives such as MBCQ have similar activity profiles (data not shown). In contrast, the treatment of 3-MA has no effect on the protein level of Beclin1 (Figure S4C). These data confirm that spautin-1 selectively reduces the levels of Vps34 complexes in mammalian cells.

To explore the mechanism by which spautin-1 reduces the levels of Vps34 complexes, we treated H4-LC3-GFP cells with MBCQ or spautin-1 in the presence or absence of CHX. As shown in Figure 3G, the addition of spautin-1 with CHX reduced the levels of Beclin1 and Vps34 compared to that of CHX alone, suggesting that spautin-1 may promote the degradation of the class III PI3 kinase complexes. To further examine this possibility, we treated H4-LC3-GFP cells with spautin-1 in the presence of MG132 or NH_4Cl to inhibit proteasomal or lysosomal degradation, respectively. MG132 but not NH_4Cl inhibited the reduction of Beclin1 induced by spautin-1 (Figure 3H). The addition of MG132 restored the levels of Vps34 complexes as well as that of autophagy (Figure S5A). Similar results were found with transfected GFP-Beclin1 in 293T cells (Figure S5B). These results suggest that spautin-1 promotes the degradation of Beclin1 through the proteasomal pathway. Since ubiquitination represents an essential step in mediating proteasomal degradation, we tested if ubiquitination of Beclin1 was increased in cells treated with spautin-1. As shown in Figure 3I, the treatment of spautin-1 promoted the ubiquitination of Beclin1 without an obvious effect on the global levels of ubiquitination. Taken together, we conclude that spautin-1 inhibits autophagy by selectively promoting the degradation of the class III PI3 kinase complexes via the proteasomal pathway.

Identification of the Deubiquitinating Enzymes for Vps34 Complexes

Since ubiquitination of proteins plays a critical role in mediating proteasomal degradation, we hypothesize that spautin-1 targets deubiquitinating enzyme(s) (DUBs) which normally function to negatively regulate the ubiquitination of Vps34 complexes. This follows from the common finding that a small molecule is more likely to be an inhibitor than an activator. To directly test this hypothesis, we screened a collection of 127 siRNAs targeting Human Deubiquitinating Enzymes from the Dharmacon library SMART pools for inhibition of autophagy using H4-LC3-GFP cells as an assay. We found that only knockdown of USP10 or USP13 showed a consistent effect of reducing the levels of endogenous Vps34, Beclin1, Atg14L, p150 and UVRAG (Figures 4A and 4B). Interestingly, the treatment of spautin-1 also reduced the levels of USP10 and USP13, but not USP14, a DUB involved in regulating proteasome function (Lee et al., 2010), or Rubicon, a negative regulator of type III PI3 kinase

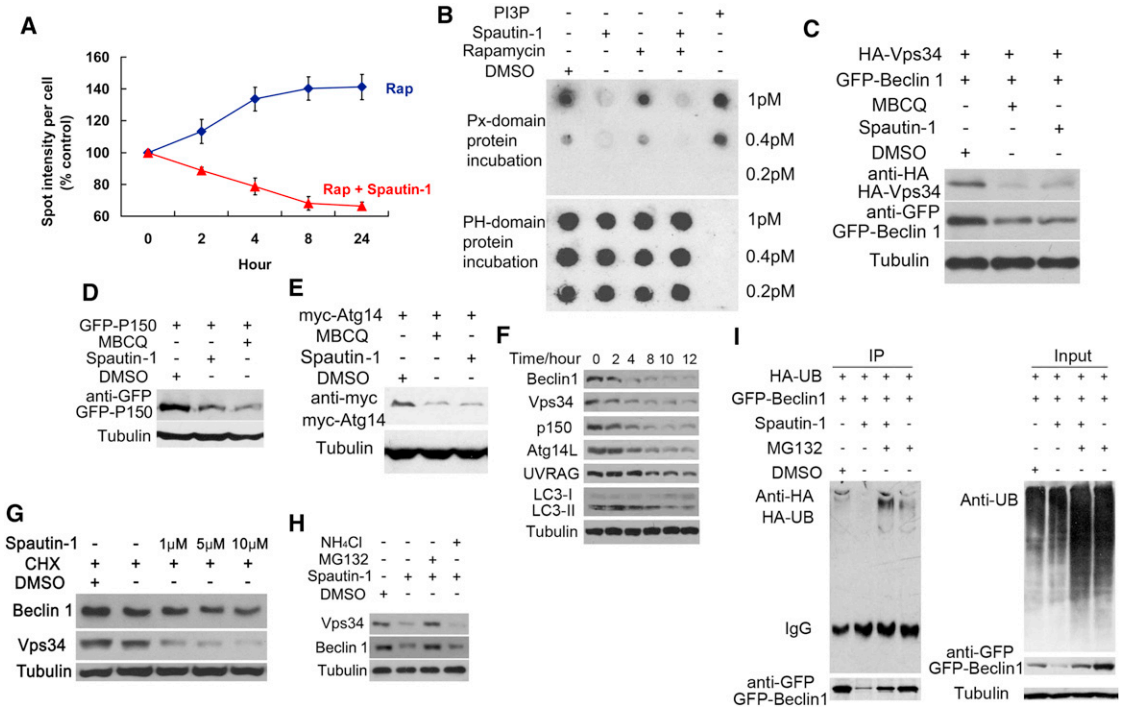

Figure 3. Spautin-1 Reduces the Levels of PtdIns3P by Promoting the Degradation of Vps34 Complexes

(A) H4-FYVE-RFP cells were treated with rapamycin (0.2 μM) and/or spautin-1 (10 μM) as indicated. The image data are expressed as % of control vehicle treated cells. 1000 cells were analyzed per treatment condition. Rap = rapamycin.

(B) MEF cells were treated with DMSO (1‰), rapamycin (0.2 μM), spautin-1 (10 μM) as indicated for 4 hr. The lipids were extracted and applied onto polyvinylidene fluoride membrane. The commercial PtdIns3P was spotted as indicated for controls. The levels of PtdIns3P were detected using GST-PX-p40 domain protein, which binds to PtdIns3P, and anti-GST antibody (top panel). The levels of PtdIns4P, detected using GST-PH-FAPP-1 domain protein which binds to PtdIns4P, and anti-GST antibody, were used as a loading control (bottom panel).

(C-E) 293T cells were transfected with expression vectors of HA-Vps34 and Flag-Beclin 1 (C), GFP-p150 (D), or myc-Atg14L (E). Twenty-four hours after transfection, cells were treated with DMSO (1‰), MBCQ (10 μM) or spautin-1 (10 μM) as indicated for 24 hr. The cell lysates were analyzed by western blotting using anti-HA, anti-Flag, anti-GFP, anti-myc as indicated or anti-β-tubulin (as a control).

(F) H4-LC3-GFP cells were treated with spautin-1 (10 μM) as indicated, the cell lysates were analyzed by western blotting using indicated antibodies. β-tubulin was used as a control.

(G) H4-LC3-GFP cells were treated with CHX (10 μM) or spautin-1 at indicated concentrations for 12 hr. DMSO (1‰) was used as a negative control. The cell lysates were analyzed by western blotting using anti-Beclin1, anti-Vps34, or anti-β-tubulin (as a control).

(H) H4-LC3-GFP cells were incubated with MG132 (10 μM) or NH_4Cl (10 mM) with or without spautin-1 (10 μM) for 6 hr. The cell lysates were analyzed by western blotting using using indicated antibodies. β-tubulin was used as a control.

(I) 293T cells were transfected with GFP-Beclin1 and HA-Ub expression vectors. Twenty-four hours after transfection, cells were treated with spautin-1 (10 μM) for 24 hr and MG132 (5 μM) was added in the last 6 hr. The cell lysates were immunoprecipitated with anti-GFP antibody and the immunocomplexes were analyzed by western blotting using anti-HA antibody. All error bars indicate STD. See also Figure S4.

(Matsunaga et al., 2009; Zhong et al., 2009) (Figure 4C). Similarly, the treatment of MEF cells with spautin-1 also led to a time-dependent reduction in the levels of USP10, USP13, Vps34 complexes and autophagy (Figure S5C). In addition, we compared the effects of spautin-1 on HeLa and Bcap-37 cells under normal culture condition and autophagy induction conditions (Figures S5D and S5E). Interestingly, we found that the reduction in the levels of Vps34 complexes in Bcap-37 cells was significantly stronger under autophagy induction conditions than that under normal culture conditions, where autophagy levels are low.

Because the reductions in the levels of USP10 and USP13 in H4-LC3-GFP cells treated with spautin-1 appeared later than the reductions in the levels of Vps34 complexes and autophagy (Figure 4C), the reduced levels of USP10 and USP13 are unlikely to be the primary reason for the ability of spautin-1 to reduce the levels of PtdIns3P and inhibit autophagy. Since the treatment with spautin-1 increases the ubiquitination levels of Beclin1 and knockdown of USP10 or USP13 reduces the levels of Vps34 complexes, we considered the possibility that spautin-1 targets USP10 and USP13 mediated the deubiquitination of Vps34 complexes. We first examined the ability of USP10 and USP13 to mediate the deubiquitination of Vps34 complexes. We found that the overexpression of USP10 was highly effective in reducing the levels of ubiquitinated Beclin1, and this effect was inhibited in the presence of spautin-1 (Figure 4D). Similarly, the overexpression of USP13 reduced the levels of ubiquitinated Beclin1 which was inhibited by spautin-1 (Figure 4E). On the other hand, overexpression of USP10 or USP13 had no obvious effects on the ubiquitination levels of overexpressed Vps34,

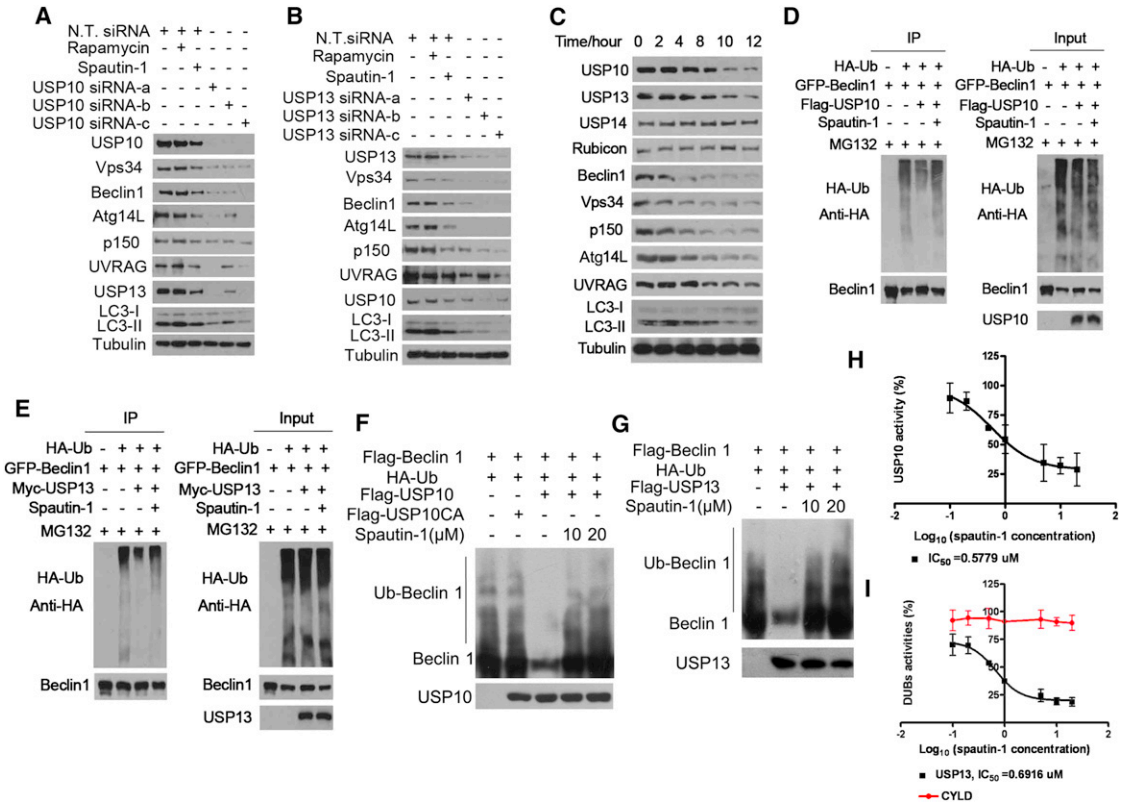

Figure 4. Spautin-1 Inhibits the Deubiquitination of Vps34 Complexes

(A) and (B) H4-LC3-GFP cells were transfected with indicated siRNAs for 72 hr or treated with rapamycin (0.25 μM) or spautin-1 (10 μM) as indicated, the cell lysates were analyzed by western blotting using indicated antibodies. β-tubulin was used as a control.

(C) H4-LC3-GFP cells were treated with spautin-1 (10 μM) as indicated, the cell lysates were analyzed by western blotting using indicated antibodies. β-tubulin was used as a control.

(D and E) 293T cells were transfected with indicated expression vectors for 12 hr, incubated with MG132 (10 μM), with or without spautin-1 (10 μM) for 4 hr, the cell lysates were immunoprecipitated with anti-Beclin1 and the immunocomplexes were analyzed by western blotting using anti-HA antibody.

(F) and (G) Ubiquitinated Beclin1 was incubated with immunopurified Flag-USP10, Myc-USP13, or Flag-USP10CA, with or without spautin-1 for 2 hr in vitro in deubiquitinating buffer. The western blot was blotted with anti-Beclin1 antibody.

(H) and (I) Proteins indicated purified from 293T cells and different concentrations of spautin-1 (20 μM to 100 nM) were mixed and incubated for 30 min. Ub-AMC was then added to each well and incubated for another 45 min. The final concentrations of every protein and Ub–AMC were 20 nM and 0.8 μM, respectively. Ub–AMC hydrolysis was measured.

All error bars indicate STD. See also Figure S5.

Atg14L, p150, and UVRAG (Figures S6A–S6H). Taken together, these results suggest that Beclin1 is the primary target of USP10 and USP13.

To directly test if spautin-1 can inhibit the deubiquitinating activity of USP10 and USP13, we tested the activity of isolated USP10 and USP13 on ubiquitinated Beclin1 in vitro. As shown in Figures 4F and 4G, the coincubation of ubiquitinated Beclin1 with USP10 or USP13 but not a catalytically inactive USP10 mutant reduced the levels of Beclin1 ubiquitination. Furthermore, the presence of spautin-1 inhibited the deubiquitination of Beclin1 mediated by USP10 and USP13. In contrast, spautin-1 had no effect on CYLD-mediated deubiquitination of RIP1 in vitro (data not shown). To further confirm this result, we developed an in vitro deubiquitination assay using Ub-AMC (the C-terminal derivatization of ubiquitin with 7-amino-4-methylcoumarin), which is a fluorogenic substrate for deubiquitinating enzymes (DUBs) (Dang et al., 1998). Using this assay, we found that spautin-1 inhibited USP10 and USP13 with IC_{50} of ~0.6-0.7 μM while having no inhibitory activity toward CYLD which is also a member of ubiquitin specific peptidase family (Figures 4H and 4I). Thus, spautin-1 is an inhibitor of the deubiquitinating activity of USP10 and USP13. Our results suggest that inhibition of USP10 and USP13 by spautin-1 promotes the ubiquitination and degradation of Vps34 complexes which in turn leads to a reduction in the levels of PtdIns3P and consequent inhibition of autophagy.

Regulation of USP10 and USP13 by Vps34 Complexes

Unexpectedly, we found that the knockdown of Beclin1 or Vps34 could also reduce the endogenous levels of USP10 and USP13 (Figures 5A and 5B). This suggests that Vps34 complexes may be able to regulate their own levels by stabilizing their cognate

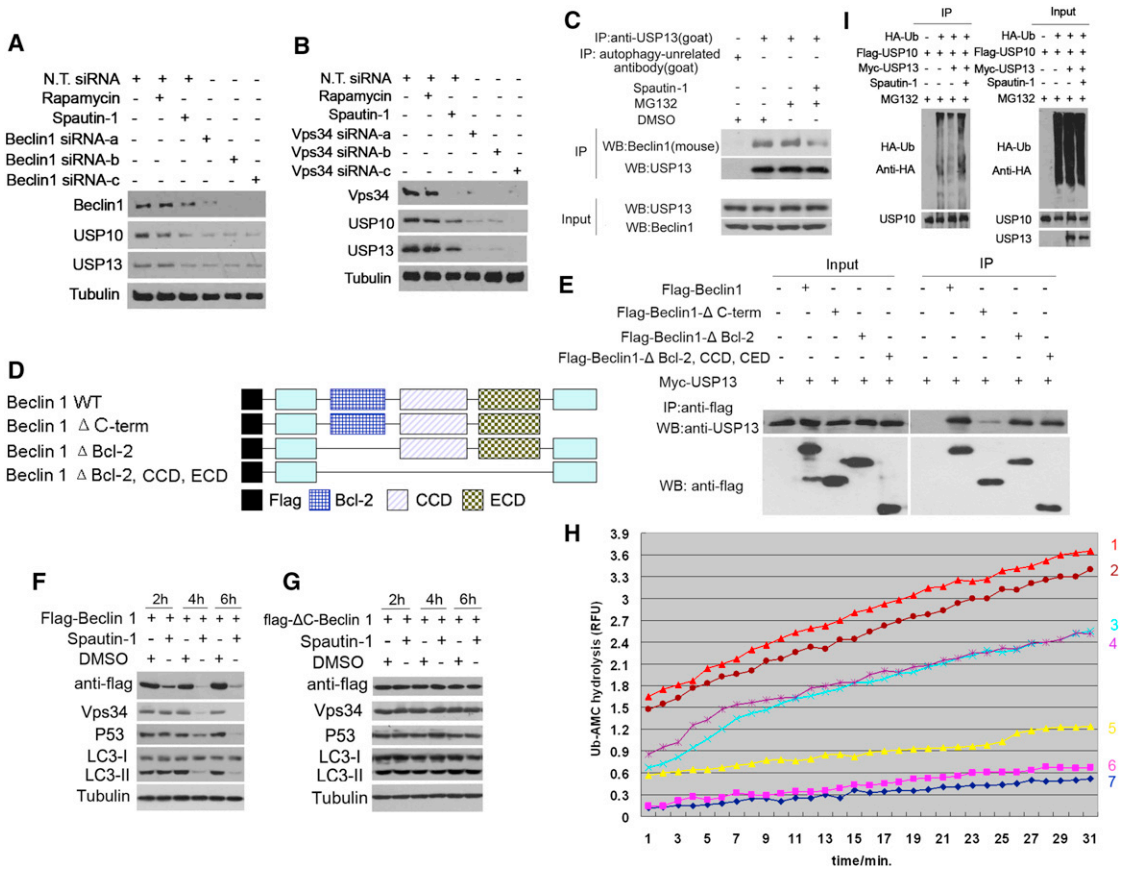

Figure 5. Regulation of USP13 by Vps34 Complexes

(A and B) H4-LC3-GFP cells were transfected with indicated siRNAs for 72 hr or treated with rapamycin (0.25 μM) or spautin-1 (10 μM) for 4 hr, the cell lysates were analyzed by western blotting using indicated antibodies. β-tubulin was used as a control.

(C) H4-LC3-GFP cells were treated with MG132 (10 μM) and spautin-1 (10 μM) for 6 hr. The cell lysates were immunoprecipitated with anti-USP13 antibody and the immunocomplexes were analyzed by western blotting using anti-Beclin1 antibody.

(D) A schematic diagram of Beclin1 truncation mutants used in (E).

(E) 293T cells were transfected with Myc-USP13, Flag-Beclin1, Flag-Beclin1-ΔC-term, Flag-Beclin1-ΔBD, Flag-Belin1-ΔBD,CCD,CED as indicated for 24 hr. The cell lysates were immunoprecipitated with anti-flag antibody and the immunocomplexes were analyzed by western blotting using anti-USP13 antibody.

(F and G) 293T cells were transfected with flag-Beclin1 or flag-ΔC-Beclin1 for 24 hr, and then treated with spautin-1(10 μM) as indicated. The cell lysates were assayed by anti-flag, anti-Vps34, anti-p53, anti-LC3, β-tubulin (loading control) as indicated.

(H) Flag-Beclin1, Flag-USP10 and Myc-USP13 proteins were isolated from 293T cells individually transfected with the relevant expression constructs by immunoprecipitation followed by extensive washing (12x) and elution with tag peptides. Deubiquitinating activities of indicated proteins were analyzed using Ub-AMC assay. Line 1: Myc-USP13, Flag-USP10 and Flag-Beclin1; Line 2: Myc-USP13 and Flag-Beclin1; Line 3: Flag-USP10 and Flag-Beclin1; Line 4: Myc-USP13 and Flag-USP10; Line 5: Myc-USP13; Line 6: Flag-USP10; Line 7: Flag-Beclin1.

(I) 293T cells were transfected with indicated expression vectors for 12 hr, incubated with MG132 (10 μM) in the presence or absence of spautin-1 (10 μM) for an additional 4 hr. The cell lysates were immunoprecipitated with anti-USP10 antibody and the immunocomplexes were analyzed by western blotting using anti-HA antibody.

See also Figure S6.

deubiquitinating enzymes including USP10 and USP13. This effect is not likely mediated through PtdIns3P, the product of Vps34 complexes, as the treatment of 3-MA which inhibits the kinase activity of class III PI3 kinase had no effect on the levels of USP10 or USP13 (data not shown). Thus, Vps34 complexes have the surprising role of regulating the stability of USP10 and USP13.

To determine the mechanism by which Vps34 complexes regulate the stability of USP13 and USP10, we examined the possibility that Beclin1 may interact with USP10 and USP13. We found that endogenous Beclin1 can interact with USP13 and the interaction was reduced in the presence of spautin-1 (Figure 5C). However, the interaction of Beclin1 and USP10 was considerably weaker (data not shown). These data suggest that Beclin1 may closely interact with USP13, whereas its interaction with USP10 is indirect or transient in nature.

To further characterize the interaction of USP13 with Beclin1, we determined the domains of Beclin1 that interact with USP13 (Figure 5D & E). Different truncation mutants of Beclin1 were coexpressed with USP13 in 293T cells and the interaction of

USP13 with different Beclin1 mutants was analyzed by coimmunoprecipitation. A C-terminal deletion mutant of Beclin1 (ΔC-Beclin1) showed significantly reduced binding with USP13, suggesting the C terminus of Beclin1 is important for the interaction. We further compared the effect of spautin-1 in 293T cells expressing ΔC-Beclin1 mutant or full length Beclin1 (Figures 5F and 5G). Interestingly, we found that not only was the ΔC-Beclin1 mutant resistant to spautin-induced degradation, but the expression of ΔC-Beclin1 mutant significantly blocked the effect of spautin-1 in inhibiting autophagy and inducing the degradation of Vps34. Since ΔC-Beclin1 can bind to Vps34 (Furuya et al., 2010) but not USP13, this experiment suggests that the interaction of Beclin1 and USP13 is critically important for regulating the stability of Vps34 complexes in response to spautin-1 treatment.

To directly examine the mechanism by which Beclin1 regulates USP10 and USP13, we determined the effects of their interaction on the deubiquitinating activities in vitro using Ub-AMC as a substrate. As shown in Figure 5H, the DUB activities of USP10 or USP13 were comparatively low when incubated alone with Ub-AMC. Interestingly, the DUB activities were significantly increased when USP13 and USP10 coincubated together or with Beclin1 or all 3 proteins together, suggesting the DUB activity can be significantly enhanced when USP13 interacts with its substrate Beclin1 or USP10. Thus, reduced levels of USP10 and USP13 in the presence of spautin-1 or with *beclin1* knockdown may be due to their increased ubiquitination and degradation through the proteasome pathway. Consistent with this possibility, the effect of spautin-1 on the levels of USP10 and Vps34 complexes can be fully restored in the presence of MG132 (Figure S5A). Furthermore, the effect of Beclin1 knockdown on reduced levels of USP10 and USP13 can also be inhibited by MG132 (Figure S7B).

Deubiqutination of USP10 by USP13

Since the treatment of spautin-1 also led to reduced levels of USP10, which was inhibited by the addition of MG132 (Figure S5A), it is likely that the levels of USP10 and USP13 are also regulated by ubiquitination. Interestingly, knockdown of either USP10 or USP13 led to reductions in the levels of the other (Figures 4A and 4B). Thus, we considered the possibility that USP10 and USP13 may regulate deubiquitination of each other. Consistent with this possibility, the ubiquitination levels of USP10 were reduced when cells were cotransfected with an expression vector of USP13 and the addition of spautin-1 inhibited the deubiquitination of USP10 by USP13 (Figure 5I). On the other hand, coexpression of USP10 with USP13 has a much less pronounced effect on ubiquitination of USP13 (data not shown). These results suggest that USP13 may directly regulate the deubiquitination of USP10; however, USP10 may regulate USP13 indirectly perhaps by affecting the levels of Vps34 complexes. Since USP10 mediates the deubiquitination of Beclin1 and reduced levels of USP10 leads to increased ubiquitination and degradation of Vps34 complexes, reduced levels of Vps34 complexes as a result of USP10 reduction may in turn lead to destabilization of USP13.

Our data supports an interactive regulatory relationship of USP10 and USP13 with Vps34 complexes. We propose that USP10 and USP13 mediate the deubiqutination of Vps34 complexes to regulate the levels of class III PI3 kinase. Furthermore, Beclin1 also interacts with USP13 and regulates the stability of USP13. Since USP13 can also deubiquitinate USP10, regulating the stability of USP13 by Beclin1 provides a mechanism for Beclin1 to control the stability of USP10. Thus, our data suggest that the levels of Vps34 complexes may be coupled to the levels of USP10 and USP13.

Regulation of p53 via Vps34 Complexes and Deubiquitination

Since USP10 is known as a deubiquitinating protease of p53 (Yuan et al., 2010), inhibition of USP10 by spautin-1 may promote the degradation of p53. Consistent with this possibility, the treatment of spautin-1 led to a reduction in the levels of p53 that was inhibited in the presence of MG132 (Figure S5A). Furthermore, spautin-1 induced reduction in the levels of p53 was inhibited with knockdown of MDM2, the major E3 ubiquitin ligase for p53 (Figure 6A). On the other hand, knockdown of Mdm2 had no effect on spautin-1 induced reduction of USP10, USP13, Vps34 or Beclin1. In addition, we found that knockdown of USP10, USP13, Beclin1, Vps34, p150, UVRAG, Atg14L all led to reduction in the levels of p53 (Figures 6B–6E; Figure S7A). Thus, the cellular levels of p53 may be coordinately regulated with that of Vps34 complexes via deubiquitinating enzymes such as USP10 and USP13. Finally, consistent with Beclin1 being the primary target of USP10 and USP13, the expression of ΔC Beclin1, which behaves as a dominant negative in inhibiting the loss of Vps34 complexes and autophagy, also inhibited the reduction of p53 induced by spautin-1 (Figure 5F and 5G).

Since our model predicts that the levels of class III PI3 kinase should be correlated with that of p53, we examined the levels of p53 in *BECN1*+/− mice. As shown in Figure 6F, the levels of Beclin1 in newborn *BECN1*+/− mice are approximately half of that in wt mice. Consistent with a coordinated regulation of Vps34 complex components, the levels of Vps34, Atg14L, p150 and UVRAG are also significantly reduced in *BECN1*+/− tissues. Interestingly, as predicted by our model, the levels of USP10 and p53 in the heart, lung and liver of newborn *BECN1*+/− mice are correspondingly reduced. The levels of USP13 could not be examined currently due to a lack of antibody that can recognize murine USP13. The levels of LC3II in *BECN1*+/− liver are reduced compared to that of wt. On the other hand, the reduction of LC3II in heart and lung of *BECN1*+/− mice is not as obvious as that in liver. The reduced levels of p53 provide an important molecular mechanism contributing to the increased tumorigenesis in *BECN1*+/− mice.

To further characterize the effect of spautin-1 on p53, we examined the effect of spautin-1 on the cytoplasmic and the nuclear levels of p53 and found that the treatment of spautin-1 can reduce both nuclear and cytoplasmic p53 (Figure S7C). Furthermore, we found that the effects of spautin on the levels of Vps34 complexes and autophagy could still be observed in SKOV-3 ovarian cancer cell line which is null for p53 (Figure S7D). These results are consistent with the target of spautin-1 being upstream and independent of p53.

Taken together, our data suggest a model of regulatory relationship between class III PI3 kinase and p53 via protein interaction and deuqibuitination and the mechanism by which the

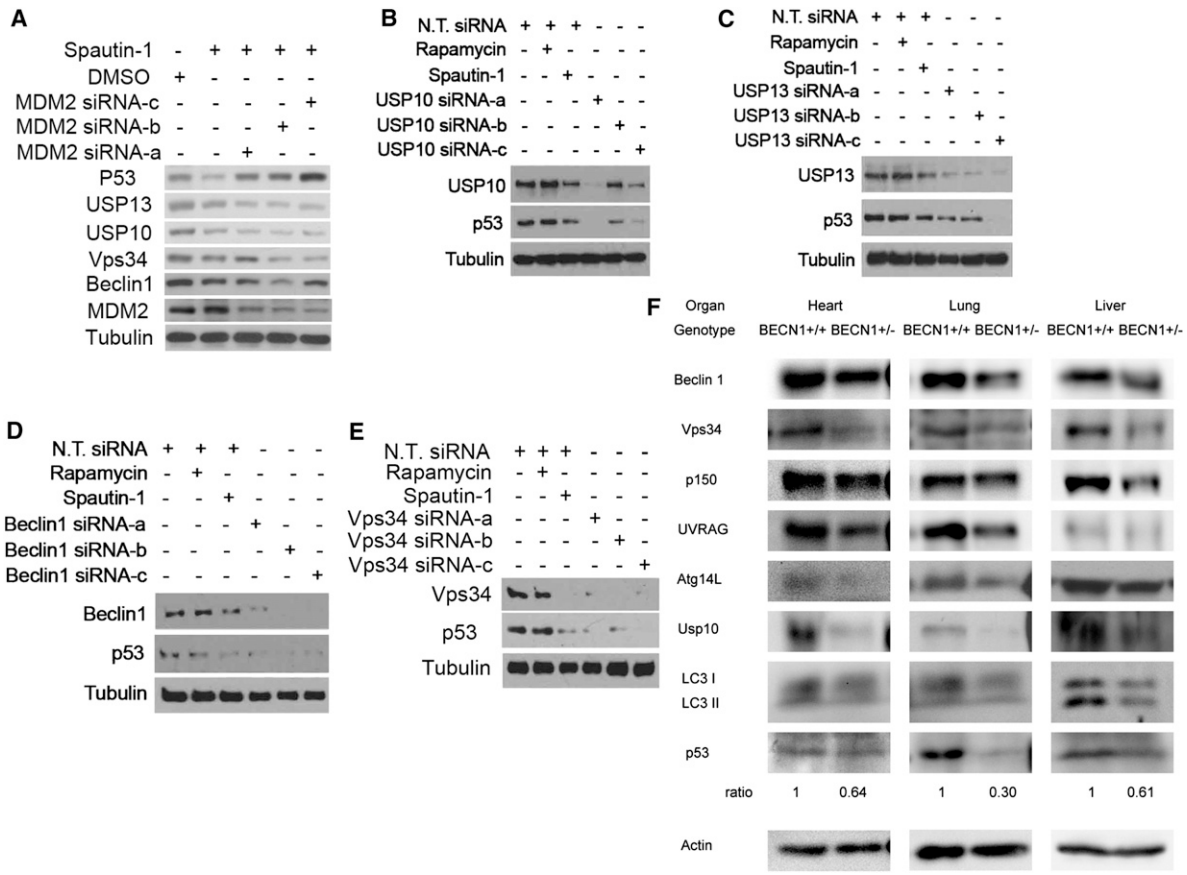

Figure 6. Regulation of p53 by Vps34 Complexes, USP10 and USP13

(A-E) H4-LC3-GFP cells were transfected with indicated siRNAs for 72 hr and treated with rapamycin (0.25 μM) or spautin-1 (10 μM) for 4 hr. The cell lysates were analyzed by western blotting using indicated antibodies. Anti-β-tubulin is a loading control.

(F) Heart, lung and liver tissues of newborn *BECN1*+/+ and *BECN1*+/− mice were isolated and analyzed by western blotting using indicated antibodies. Anti-actin was used as a loading control.

Also see Figure S7.

treatment with spautin-1 leads to the reduced levels of Vps34 complexes and p53 (Figure 7).

DISCUSSION

In this study, we describe a potent small molecule inhibitor of autophagy, named spautin-1, that targets the deubiquitination activity of USP10 and USP13. Using spautin-1 as a tool, we demonstrate that the ubiquitination and degradation of Vps34 complexes are regulated by two ubiquitin-specific peptidases, USP10 and USP13. Inhibiting deubiquitination of Vps34 complexes by spautin-1 leads to increased ubiquitination and degradation of class III PI3 kinase complexes through the proteasomal pathway. Furthermore, our study demonstrates a physiological mechanism for regulating the class III PI3 kinase via protein deubiquitination. Since class III PI3 kinase plays an important role in regulating multiple intracellular vesicular trafficking events including autophagy and endocytosis, the ability of USP10 and USP13 to regulate the stability of Vps34 complexes provides a molecular mechanism for ubiquitination and proteasomal degradation to control intracellular vesicular trafficking. Unlike that of class I and class II PI3 kinases which need to be activated through receptor signaling, the activity of class III PI3 kinase is believed to be constitutive (Lindmo and Stenmark, 2006). Thus, regulating the protein levels of class III PI3 kinase might provide an important mechanism for controlling the constitutively active class III PI3 kinase and intracellular levels of PtdIns3P. Our recent genome-wide siRNA screen on autophagy demonstrated a prominent role of class III PI3 kinase in regulating autophagy (Lipinski et al., 2010). It will be interesting in future to examine if regulating deubiquitination and ubiquitination of Vps34 complexes provides a general mechanism for controlling the constitutively active class III PI3 kinase activities under different physiological conditions. Consistent with the regulation of this deubiquitination mechanism, we found that the effect of spautin-1 on the levels of Vps34 complexes are dramatically enhanced in Bcap-37 cells under glucose-free condition, suggesting that the deubiquitination of Vps34 complexes may be under the control of nutritional availability. Thus, inhibiting the deubiquitination of Vps34 complexes might

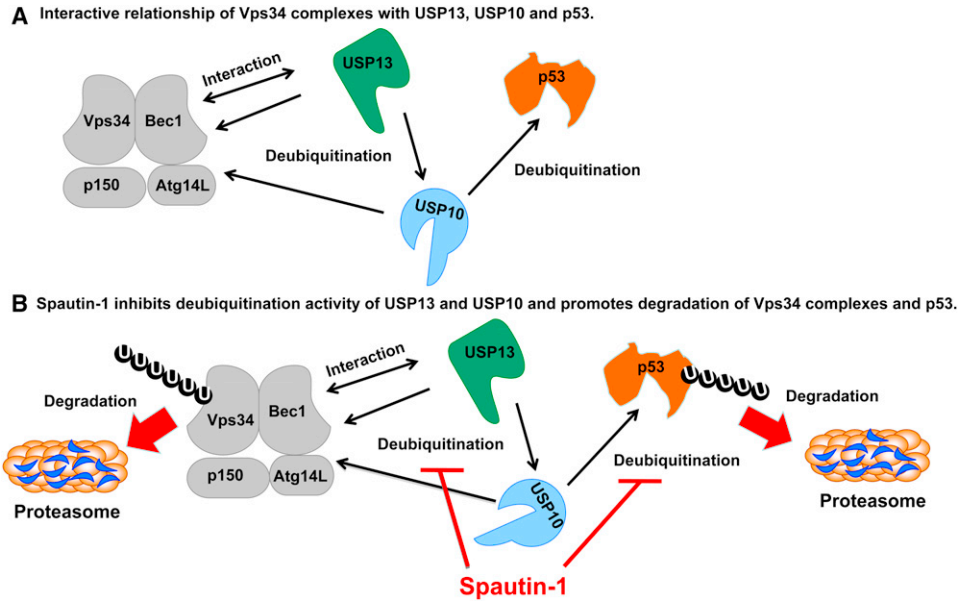

Figure 7. A Model: USP10 and USP13 Mediate the Deubiquitination of Vps34 Complexes and p53

(A) In cells treated with spautin-1, USP10 and USP13 are inhibited which leads to increased ubiquitination and degradation of Beclin1 in Vps34 complexes and p53.

(B) USP13 interacts with Beclin1 in Vps34 complexes which provides a mechanism for Vps34 complexes to regulate the deubiquitination activity of USP13. USP13 also mediates the deubiquitination of USP10 which explains why knockdown of USP13 also leads to increased degradation of USP10. On the other hand, knockdown of USP10 leads to the loss of Vps34 complexes which might in turn destabilizes USP13.

provide a strategy for developing autophagy inhibitors as an anticancer therapy.

USPs are cysteine proteases containing conserved regions in their amino acid sequence surrounding the Cys, His and Asp/Asn residues that form the catalytic triad. From the structural studies of a number of USP family members, it has been noted that the USP catalytic domains are often not appropriately aligned without binding to their substrates (Komander, 2010). That is, the catalytic Cys in USP7 shifts from catalytically inactive position to an active position where it interacts with the catalytic His only when binding to ubiquitin. On the other hand, although the catalytic machineries of USP14 and USP8 are properly aligned for catalysis in the absence of ubiquitin, the ubiquitin binding sites are blocked by the ubiquitin-binding surface loops (Hu et al., 2005). In addition, the Fingers domain of USP8, which is important for binding to ubiquitin, folds inward which blocks the ubiquitin binding site when not interacting with its substrates. Although no structural information for USP13 and USP10 is currently available, the enhanced DUB activity when USP13 interacts with USP10 or when they interact with Beclin1 suggest that the interaction of USP13 and USP10 with each other or with their substrates can lead to changes in their conformation which may be critical for the catalytic activities. This provides a possible model and mechanism for the close interactive regulatory relationship between USP13/USP10 with Vps34 complexes to explain why knockdown of USP13/USP10 or Vps34 complexes lead to reduced levels of the others.

We demonstrate that USP10 and USP13 can both mediate the deubiquitination of Beclin1. Since the stabilities of the core components of Vps34 complexes are codependent upon each other (Itakura et al., 2008), regulating deubiquitination of Beclin1 may be sufficient to control the levels of whole complex. On the other hand, our study also demonstrates that Vps34 complexes can regulate their own levels by a feedback control of USP13. Since the interaction of USP13 and Beclin1 is detectable by coimmunoprecipitation, we propose that Beclin1 may have close interaction with USP13. On the other hand, the interaction of Beclin1 and USP10 is consistent with that of enzyme/substrate which is expected to be weak and transient in nature. Most DUBs with resolved structures show that the enzymes are in an unproductive conformation before binding to the substrates. These inactive states might result from the blocking of the active site by loops or a misalignment of catalytic triads. Thus, binding to Beclin1 may trigger a major change in the conformation of USP13 to allow catalysis.

Our study demonstrates that class III PI3 kinase is an important tumor suppressor. The role of *beclin1* as a haploid-insufficient tumor suppressor is well-established; however, it has been unclear how might a reduction in *beclin1* expression can have such a dramatic impact on genomic instability and tumorigenesis (Karantza-Wadsworth et al., 2007). Our study demonstrates that a reduction of *beclin1* expression leads to a reduced p53 level by increasing its ubiquitination, providing an important molecular mechanism contributing to the role of *beclin1* as a haploid-insufficient tumor suppressor that is frequently monoallelically lost in human breast, ovarian, and prostate cancers (Liang et al., 1999; Qu et al., 2003; Yue et al., 2003).

Recently, using mutant mice with tissue-specific Atg5 or Atg7 deficiency, Takamura et al. showed that multiple benign tumors developed from autophagy deficient liver, but not in other tissues

(Takamura et al., 2011). Thus, it is unlikely that increased rate of tumorigenesis in *BECN1*+/− mice is due to autophagy deficiency as assumed originally. Since Beclin1 has been shown to interact with Bcl-2, it has also been proposed that decreased levels of Beclin1 in *BECN1*+/− cells may promote the activity of Bcl-2 to increase cell survival which in turn promotes tumorigenesis (Pattingre et al., 2005). While our model does not rule out of a potential contribution of Bcl-2 or autophagy deficiency from promoting tumorigenesis in *BECN1*+/− mice, the reduced levels of p53 as a result of reduction in Beclin1 might provide a mechanism to promote genomic instability which in turn leads to tumorigenesis. The ability of Beclin1 to regulate the levels of p53 provides a mechanism underlying the observations that monoallelic loss of *beclin1* is sufficient to lead to DNA damage and genomic instability via gene amplification (Karantza-Wadsworth et al., 2007).

Consistent with the contribution of p53 deficiency to increased tumorigenesis in *beclin1* heterozygous background, the tumor spectra of *TP53*+/− mice and *BECN1*+/− mice strongly overlap: the highest frequencies of tumors in both *TP53*+/− and *BECN1*+/− mice are lung carcinoma, hepatoma and lymphoma (Jacks et al., 1994; Qu et al., 2003). Furthermore, the *beclin1* gene is frequently monoallelically deleted in human sporadic ovarian, prostate and breast cancers similar to that of p53 mutations (http://www-p53.iarc.fr). The similarities in tumor spectra of *BECN1*+/− mice and *TP53*+/− mice suggest that reduced p53 levels play an important role in promoting tumorigenesis in *BECN1*+/− mice. Since the stability of the components of Vps34 complexes are largely codependent upon each other, reduced expression of other components of Vps34 complexes, including Vps34, p150, Atg14L and UVRAG, also leads to reduced levels of p53. Thus, our data suggest that all components of Vps34 complexes can regulate the levels of p53.

Curiously, although monoallelic loss of *beclin1* is frequently observed in breast, ovarian and prostate cancers, the loss of heterozygocity of *beclin1* was not commonly observed (Liang et al., 1999; Qu et al., 2003; Yue et al., 2003). Thus, *beclin 1* might not represent a "conventional" tumor suppressor such as Rb that satisfies the "Knudson two-hit hypothesis" criteria for classification as a tumor suppressor gene which indicates that it is necessary to demonstrate loss of both alleles, via either deletion or the presence of inactivating mutations (Knudson, 1971). Since *TP53*−/− mice are viable while *BECN1*−/− mice are early embryonic lethal, Vps34 complexes must provide a wider range of vital cellular functions than controlling p53 protein levels. Thus, while a reduction in *beclin1* expression might promote tumorigenesis by reducing the levels of p53, a complete loss of *beclin1* might negatively impact the development of certain tumors at least as a complete loss of *beclin1* leads to early embryonic lethality (Qu et al., 2003; Yue et al., 2003) and might be required for cell viability at least for certain cell types. Thus, unlike "conventional" tumor suppressor, bi-allelic loss of *beclin1* may not promote tumorigenesis and may lead to cell death. Consistent with this possibility, in contrast to that of normal cells, selected cancer cell lines demonstrate an increased sensitivity toward spautin-1 under starvation condition, suggesting that spautin-1 may be used to synergize with selected chemotherapeutic agents to induce cancer cell death. Spautin-1 might therefore provide a potential lead compound for developing a class of autophagy inhibitors as anticancer therapy.

EXPERIMENTAL PROCEDURES

High-Throughput Image Analysis

Cells were fixed with 4% paraformaldehyde (Sigma) and stained with 3 μg/ml DAPI (Sigma). Images data were collected with an ArrayScan HCS 4.0 Reader with a 20× objective (Cellomics ArrayScan V^{TI}) for DAPI-labeled nuclei and GFP/RFP-tagged intracellular proteins.

Cell Lines and Culture Conditions

293T, MEF, HeLa, and Bcap-37 cells were cultured in DMEM media with 10% NCS. H4-LC3-GFP, H4-FYVE-RFP and MDCK cells were cultured in DMEM supplemented with 10% FBS and 1 X Na pyruvate (Invitrogen). Hs578Bst cells were cultured in Hybri-Care Medium (ATCC), supplemented with 30 ng/ml mouse EGF and 10% FBS. For starvation experiments, cells were cultured in DMEM supplemented with 10% serum without Glucose (GIBCO).

Antibodies

Rabbit polyclonal antibody anti-USP10, anti-USP13,anti-UVRAG,anti-Vps34 and anti-p53, were from Abcam. Rabbit polyclonal antibody anti-LC3B and mouse monoclonal antibody anti-β-tubulin were from sigma. Monoclonal antibodies anti-flag, anti-Myc and anti-HA were from Abmart. Rabbit polyclonal antibody anti-Beclin1 was from Santa Cruz. Polyclonal antibody anti-Atg14L was from MBL.

Protein-Lipid Blot Assay

Protein-lipid blot assays were carried out as reported (Dowler et al., 2002; Gozani et al., 2003). Briefly, lipids extracted from a 100 mm plate was spotted onto Hybond C-extra membrane (Amersham) and allowed to dry overnight in the dark. The membrane was incubated with lipid blocking buffer (1% BSA in TBST) for 1 hr, washed once in TBST for 30 min, and incubated with protein buffer (1 μg GST-tagged protein per 1 ml TBST with 1% BSA) overnight at 4C. Then the membrane was washed again in TBST for four times at 30 min each, incubated with anti-GST (Sigma) in 1% BSA buffer for 4 hr, washed in TBST for four changes with 5 min each, incubated with secondary antibody for 1 hr, and washed in TBST for four changes with 5 min each. All incubations were at room temperature unless noted otherwise. The signals were visualized with ECL.

In Vitro Deubiquitination Assay

In vitro deubiquitination assay was carried out using a similar protocol as described in (Yuan et al., 2010). Ubiquitinated Beclin1 was isolated from 293T cells transfected with expression vectors for HA-UB and FLAG-Beclin1. After Incubation with proteasome inhibitor MG132 (25 μM) and a pan DUB inhibitor G5 (25 μM) for 6 hr, ubiquitinated Beclin1 was purified from the cell extracts with anti-FLAG-affinity column in FLAG-lysis buffer (50 mM Tris-HCl [pH 7.8], 137mM NaCl, 10mM NaF, 1mM EDTA, 1% Triton X-100, 0.2% Sarcosyl, 1mM DTT, 10% glycerol and fresh proteinase inhibitors). After extensive washing with the FLAG-lysis buffer, the proteins were eluted with FLAG-peptides (Sigma). The recombinant Flag-USP10 and USP10CA were expressed in 293T cells and purified using FLAG affinity column and eluted with FLAG-peptide. For in vitro deubiquitination assay, ubiquitinated Beclin1 protein was incubated with recombinant USP10 in the deubiquitination buffer (50 mM Tris-HCl [pH 8.0], 50mM NaCl, 1mM EDTA, 10mM DTT, 5% glycerol) for 2 hr at 37°C.

SUPPLEMENTAL INFORMATION

Supplemental Information includes Extended Experimental Procedures, seven figures, and one table and can be found with this article online at doi:10.1016/j.cell.2011.08.037.

ACKNOWLEDGMENTS

We thank Dan Finley, Bruce Yankner, Zhujun Yao, Dana Christofferson, Dimitry Ofengeim, and Bénédicte Py for comments on the manuscript; Dr. Xin Xie of

the National Center for Drug Screening in Shanghai for help with the original compound screen for autophagy regulators; Dr. Wade Harper for providing expression vectors of USP10 and USP13; Dr. Zhenkun Lou for mutant expression vector for USP10; Dr. Caroline Shamu (the director of the ICCB screening facility); and David Wrobel and Stewart Rudnicki for helps with siRNA screening. This work was supported in part by a NIH Director's Pioneer Award US (to J.Y.), grants from the Chinese Academy of Sciences (KGCX2-SW-209 and KJCX2-YW-H08 [to D.M.]), the National Natural Science Foundation of China (21020102037 [to D.M.], and 90813007 [to L.Z.]) and the National Institute on Aging US (R37 AG012859 and PO1 AG027916 [to J.Y.]). M.K. is a recipient of Samsung Scholarship from South Korea. H.V.N. is supported in part by a fellowship form the Swedish Society for Medical Research (SSMF).

Received: November 29, 2010
Revised: June 24, 2011
Accepted: August 16, 2011
Published: September 29, 2011

REFERENCES

Dang, L.C., Melandri, F.D., and Stein, R.L. (1998). Kinetic and mechanistic studies on the hydrolysis of ubiquitin C-terminal 7-amido-4-methylcoumarin by deubiquitinating enzymes. Biochemistry *37*, 1868–1879.

Dowler, S., Kular, G., and Alessi, D.R. (2002). Protein lipid overlay assay. Sci. STKE *2002*, pl6.

Furuya, T., Kim, M., Lipinski, M., Li, J., Kim, D., Lu, T., Shen, Y., Rameh, L., Yankner, B., Tsai, L.H., et al. (2010). Negative regulation of Vps34 by Cdk mediated phosphorylation. Mol. Cell *38*, 500–511.

Gaullier, J.M., Simonsen, A., D'Arrigo, A., Bremnes, B., Stenmark, H., and Aasland, R. (1998). FYVE fingers bind PtdIns(3)P. Nature *394*, 432–433.

Gozani, O., Karuman, P., Jones, D.R., Ivanov, D., Cha, J., Lugovskoy, A.A., Baird, C.L., Zhu, H., Field, S.J., Lessnick, S.L., et al. (2003). The PHD finger of the chromatin-associated protein ING2 functions as a nuclear phosphoinositide receptor. Cell *114*, 99–111.

Hu, M., Li, P., Song, L., Jeffrey, P.D., Chenova, T.A., Wilkinson, K.D., Cohen, R.E., and Shi, Y. (2005). Structure and mechanisms of the proteasome-associated deubiquitinating enzyme USP14. EMBO. J. *24*, 3747–3756.

Itakura, E., Kishi, C., Inoue, K., and Mizushima, N. (2008). Beclin 1 forms two distinct phosphatidylinositol 3-kinase complexes with mammalian Atg14 and UVRAG. Mol. Biol. Cell *19*, 5360–5372.

Jacks, T., Remington, L., Williams, B.O., Schmitt, E.M., Halachmi, S., Bronson, R.T., and Weinberg, R.A. (1994). Tumor spectrum analysis in p53-mutant mice. Curr. Biol. *4*, 1–7.

Karantza-Wadsworth, V., Patel, S., Kravchuk, O., Chen, G., Mathew, R., Jin, S., and White, E. (2007). Autophagy mitigates metabolic stress and genome damage in mammary tumorigenesis. Genes Dev. *21*, 1621–1635.

Knudson, A.G., Jr. (1971). Mutation and cancer: statistical study of retinoblastoma. Proc. Natl. Acad. Sci. USA *68*, 820–823.

Komander, D. (2010). Mechanism, specificity and structure of the deubiquitinases. Subcell Biochem. *54*, 69–87.

Lee, B.H., Lee, M.J., Park, S., Oh, D.C., Elsasser, S., Chen, P.C., Gartner, C., Dimova, N., Hanna, J., Gygi, S.P., et al. (2010). Enhancement of proteasome activity by a small-molecule inhibitor of USP14. Nature *467*, 179–184.

Liang, C., Feng, P., Ku, B., Dotan, I., Canaani, D., Oh, B.H., and Jung, J.U. (2006). Autophagic and tumour suppressor activity of a novel Beclin1-binding protein UVRAG. Nat. Cell Biol. *8*, 688–699.

Liang, X.H., Jackson, S., Seaman, M., Brown, K., Kempkes, B., Hibshoosh, H., and Levine, B. (1999). Induction of autophagy and inhibition of tumorigenesis by beclin 1. Nature *402*, 672–676.

Lindmo, K., and Stenmark, H. (2006). Regulation of membrane traffic by phosphoinositide 3-kinases. J. Cell Sci. *119*, 605–614.

Lipinski, M.M., Hoffman, G., Ng, A., Zhou, W., Py, B.F., Hsu, E., Liu, X., Eisenberg, J., Liu, J., Blenis, J., et al. (2010). A genome-wide siRNA screen reveals multiple mTORC1 independent signaling pathways regulating autophagy under normal nutritional conditions. Dev. Cell *18*, 1041–1052.

MacPherson, J.D., Gillespie, T.D., Dunkerley, H.A., Maurice, D.H., and Bennett, B.M. (2006). Inhibition of phosphodiesterase 5 selectively reverses nitrate tolerance in the venous circulation. J. Pharmacol. Exp. Ther. *317*, 188–195.

Matsunaga, K., Saitoh, T., Tabata, K., Omori, H., Satoh, T., Kurotori, N., Maejima, I., Shirahama-Noda, K., Ichimura, T., Isobe, T., et al. (2009). Two Beclin 1-binding proteins, Atg14L and Rubicon, reciprocally regulate autophagy at different stages. Nat. Cell Biol. *11*, 385–396.

Pattingre, S., Tassa, A., Qu, X., Garuti, R., Liang, X.H., Mizushima, N., Packer, M., Schneider, M.D., and Levine, B. (2005). Bcl-2 antiapoptotic proteins inhibit Beclin 1-dependent autophagy. Cell *122*, 927–939.

Qu, X., Yu, J., Bhagat, G., Furuya, N., Hibshoosh, H., Troxel, A., Rosen, J., Eskelinen, E.L., Mizushima, N., Ohsumi, Y., et al. (2003). Promotion of tumorigenesis by heterozygous disruption of the beclin 1 autophagy gene. J. Clin. Invest. *112*, 1809–1820.

Schu, P.V., Takegawa, K., Fry, M.J., Stack, J.H., Waterfield, M.D., and Emr, S.D. (1993). Phosphatidylinositol 3-kinase encoded by yeast VPS34 gene essential for protein sorting. Science *260*, 88–91.

Shimizu, S., Kanaseki, T., Mizushima, N., Mizuta, T., Arakawa-Kobayashi, S., Thompson, C.B., and Tsujimoto, Y. (2004). Role of Bcl-2 family proteins in a non-apoptotic programmed cell death dependent on autophagy genes. Nat. Cell Biol. *6*, 1221–1228.

Simonsen, A., and Tooze, S.A. (2009). Coordination of membrane events during autophagy by multiple class III PI3-kinase complexes. J. Cell Biol. *186*, 773–782.

Takamura, A., Komatsu, M., Hara, T., Sakamoto, A., Kishi, C., Waguri, S., Eishi, Y., Hino, O., Tanaka, K., and Mizushima, N. (2011). Autophagy-deficient mice develop multiple liver tumors. Genes Dev. *25*, 795–800.

Wang, H., Yan, Z., Yang, S., Cai, J., Robinson, H., and Ke, H. (2008). Kinetic and structural studies of phosphodiesterase-8A and implication on the inhibitor selectivity. Biochemistry *47*, 12760–12768.

Yuan, J., Luo, K., Zhang, L., Cheville, J.C., and Lou, Z. (2010). USP10 regulates p53 localization and stability by deubiquitinating p53. Cell *140*, 384–396.

Yue, Z., Jin, S., Yang, C., Levine, A.J., and Heintz, N. (2003). Beclin 1, an autophagy gene essential for early embryonic development, is a haploinsufficient tumor suppressor. Proc. Natl. Acad. Sci. USA *100*, 15077–15082.

Zhang, L., Yu, J., Pan, H., Hu, P., Hao, Y., Cai, W., Zhu, H., Yu, A.D., Xie, X., Ma, D., et al. (2007). Small molecule regulators of autophagy identified by an image-based high-throughput screen. Proc. Natl. Acad. Sci. USA *104*, 19023–19028.

Zhong, Y., Wang, Q.J., Li, X., Yan, Y., Backer, J.M., Chait, B.T., Heintz, N., and Yue, Z. (2009). Distinct regulation of autophagic activity by Atg14L and Rubicon associated with Beclin 1-phosphatidylinositol-3-kinase complex. Nat. Cell Biol. *11*, 468–476.

EXTENDED EXPERIMENTAL PROCEDURES

Synthesis of Chemical Modulators

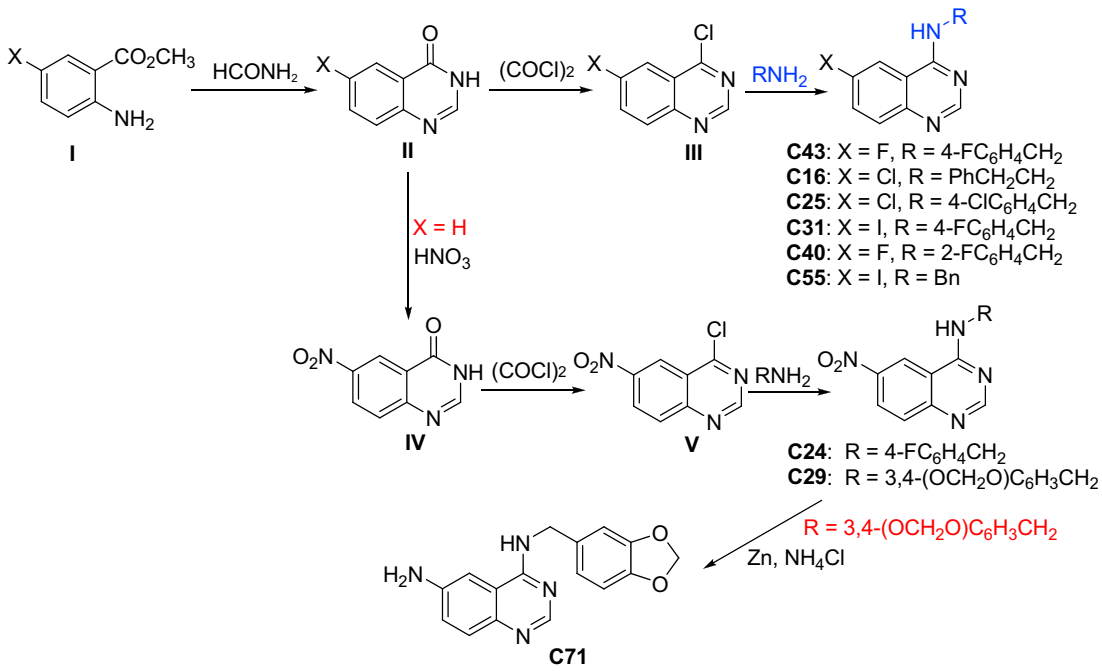

Preparation of C43

A solution of methyl 2-amino-5-fluorobenzoate (7.6 g, 0.05 mol) in formamide (40 mL) was heated at 180°C for 5 hr, then cooled down to room temperature. After vacuum filtration and washing with water, 6-fluoroquinazolin-4(3H)-one (IIa) was collected as a gray solid and dried in vacuum (9.0 g, 99%). This material was directly used in the next step.

To a solution of 6-fluoroquinazolin-4(3H)-one (760 mg, 5.2 mmol) in 1,2-dichloroethane (15 mL) was added thionyl chloride (0.67 mL, 7.8 mmol) and anhydrous DMF (0.6 mL, 7.8 mmol) under argon atmosphere. The resultant mixture was heated at 90°C for 7 hr before saturated disodium hydrogen phosphate was added at room temperature to quench the reaction. The mixture was stirred for 2 hr with cooling by ice-water, and then extracted with dichloromethane. The combined organic layers were washed with brine, dried over Na_2SO_4, and concentrated. The residue was purified via column chromatography to afford 4-chloro-6- fluoro-quinazoline (IIIa, 613 mg, 72%) as a light yellow solid.

To a solution of 4-chloro-6-fluoroquinazoline (IIIa, 50 mg, 0.304 mmol) in anhydrous THF (4 mL) was added 4-fluorobenzylamine (44 μL, 0.38 mmol) and anhydrous triethylamine (72 μL, 0.51 mmol) under argon atmosphere. The reaction was stirred at 75°C overnight. The cooled solution was concentrated and the residue was purified via column chromatography to provide C43 as a white solid (62 mg, 81%). C43: *m/z* 272.1 $(M + H)^+$, ^{1}H-NMR ($CDCl_3$, 300 MHz) δ 8.68 (s, 1H), 7.89 (m, 1H), 7.51 (m, 1H), 7.36 (m, 3H), 7.05 (t, *J* = 9.0 Hz, 2H), 5.83 (s, 1H), 4.84 (d, *J* = 5.4 Hz, 2H).

Preparation of C16

Following a similar procedure for preparing C43 from methyl 2-amino-5- fluorobenzoate, C16 was prepared from methyl 2-amino-5-chlorobenzoate. C16: *m/z* 284.1 $(M + H)^+$, ^{1}H-NMR ($CDCl_3$, 300 MHz) δ 8.68 (s, 1H), 7.78 (d, *J* = 9.0 Hz, 1H), 7.65 (d, *J* = 9.0 Hz, 1H), 7.52 (s, 1H), 7.37-7.26 (m, 5H), 5.69 (s, 1H), 3.93 (m, 2H), 3.04 (t, *J* = 6.3 Hz, 2H); HRMS (ESI): calcd for $C_{16}H_{14}N_3Cl$ 283.0876 (M^+), found 283.0876.

Preparation of C25

Following a similar procedure for preparing C43 from methyl 2-amino-5- fluorobenzoate, C25 was prepared from methyl 2-amino-5-chlorobenzoate. C25: *m/z* 303.0 $(M + H)^+$, ^{1}H-NMR ($CDCl_3$, 300 MHz) δ 8.68 (s, 1H), 7.80 (m, 1H), 7.68 (m, 2H), 7.27 (m, 4H), 5.93 (s, 1H), 4.83 (d, *J* = 5.4 Hz, 2H).

Preparation of C31

Following a similar procedure for preparing C43 from methyl 2-amino-5- fluorobenzoate, C31 was prepared from methyl 2-amino-5-iodobenzoate. C31: *m/z* 379.9 $(M + H)^+$, ^{1}H-NMR ($CDCl_3$, 300 MHz) δ 8.70 (s, 1H), 8.05 (s, 1H), 7.98 (d, *J* = 8.4 Hz, 1H), 7.58 (d, *J* = 9.0 Hz, 1H), 7.36 (t, *J* = 8.4 Hz, 2H), 7.06 (t, *J* = 8.4 Hz, 2H), 5.94 (s, 1H), 4.83 (d, *J* = 4.8 Hz, 2H); HRMS (ESI) calcd for $C_{15}H_{11}FN_3I$ 378.9986 (M^+), found 378.9982. ^{13}C-NMR (75 MHz, DMSO-d6) δ 43.5, 91.1, 115.4, 115.7, 117.2, 129.9, 130.1, 131.8, 135.8, 141.4, 148.8, 155.9, 158.5, 160.1, 163.3.

Preparation of C40

Following a similar procedure for preparing C43 from methyl 2-amino-5- fluorobenzoate, C40 was prepared from methyl 2-amino-5-fluorobenzoate. C40: *m/z* 287.1 $(M + H)^+$, ^{1}H-NMR (DMSO-d6, 300 MHz) δ 8.69 (s, 1H), 7.79 (d, *J* = 8.7 Hz, 1H), 7.69-7.66 (m, 2H), 7.46 (t, *J* = 7.8 Hz, 1H), 7.26 (m, 1H), 7.15-7.07 (m, 2H), 6.02 (s, 1H), 4,92 (d, *J* = 5.1 Hz, 2H).

Preparation of C24

A solution of quinazolin-4(3H)-one (13.2 g, 90 mmol) in sulfuric acid (50 mL) was added fuming nitric acid dropwise at −5°C. After completion of the addition, the mixture was stirred at −5°C for 2 hr and at room temperature for 1 hr. Then the mixture was poured onto crushed ice and stirred for 1 hr. Ammonia was added to regulate pH to 7∼8 at 10°C. After vacuum filtration and washing with water, 6-nitroquinazolin-4(3H)-one was collected as a yellow solid and dried in vacuum (16.51 g, 95.9%). This material was directly used in the next step.

To a solution of 6-nitroquinazolin-4(3H)-one (4.8 g, 25.2 mmol) in 1,2-dichloroethane (15 mL) was added thionyl chloride (3.24 mL, 37.8 mmol) and anhydrous DMF (2.90 mL, 37.8 mmol) under argon atmosphere. The resultant mixture was heated at 85°C for 7 hr before saturated disodium hydrogen phosphate was added at room temperature to quench the reaction. The mixture was stirred for 2 hr with cooling by ice-water, and then extracted with dichloromethane. The combined organic layers were washed with brine, dried over Na_2SO_4, and concentrated. The residue was purified via column chromatography to afford 4-chloro-6-nitroquinazoline (2.62 g, 50%) as a light yellow solid.

Following a similar procedure for preparing C43 from IIIa, C24 was prepared from 4-chloro-6-nitroquinazoline and 4-fluorobenzylamine. C24: *m/z* 299.0 $(M + H)^+$, ^{1}H-NMR (DMSO-d6, 300 MHz) δ 9.53 (t, 1H), 9.41 (d, *J* = 1.5 Hz, 1H), 8.61 (s, 1H), 8.50 (dd, *J* = 9.3, 2.4 Hz, 1H), 7.84 (d, *J* = 9.3 Hz, 1H), 7.44 (m, 2H), 7.16 (m, 2H), 4,79 (d, *J* = 5.7 Hz, 2H).

Preparation of C29

Following a similar procedure for preparing C24 from 4-fluorobenzylamine, C29 was prepared from benzo[d][1,3]dioxol-5-ylmethanamine. C29: *m/z* 325.1$(M + H)^+$, ^{1}H-NMR (DMSO-d6, 300 MHz) δ 9.46 (m, 1H), 9.41 (d, *J* = 1.8 Hz, 1H), 8.61 (s, 1H), 8.47 (dd, *J* = 9.0, 2.1 Hz, 1H), 7.84 (d, *J* = 9.3 Hz, 1H), 6.98 (s, 1H), 6.87 (m, 2H), 5.98 (s, 2H), 4,71 (d, *J* = 5.7 Hz, 2H); HRMS (ESI): calcd for $C_{16}H_{12}N_4O_4$ 324.0863 (M^+), found 324.0859; ^{13}C-NMR (75 MHz, DMSO-d6) δ 44.2, 101.3, 108.6, 108.7, 114.5, 121.1, 121.4, 126.9, 129.5, 132.8, 144.4, 146.7, 147.5, 153.2, 158.7, 160.6.

Preparation of C71

A solution of C29 (166 mg, 0.512 mmol), Zn (416 mg, 6.4 mmol) and NH_4Cl (548 mg, 10.24 mmol) in 40 ml methanol was heated at 80°C over night, then cooled to room temperature, concentrated in vacuo, and filtered, The residue was purified by column chromatography afford C71 (80 mg, 53.3%) as a white solid. C71: *m/z* 295.1 $(M + H)^+$, ^{1}H-NMR (DMSO-d6, 300 MHz) δ 8.17 (m, 2H), 7.43 (d, J = 8.7 Hz, 1H), 7.10 (m, 2H), 6.92 (s, 1H), 6.83 (s, 2H), 5.96 (s, 2H), 5.44 (s, 2H), 4.62 (d, J = 5.4 Hz, 2H).

siRNA Screen for DUBs

The primary screen tested an arrayed library of 127 siRNA pools covering all of predicted DUBs in the human genome (Dharmacon si*ARRAY* siRNA library, Thermo Fisher Scientific, Lafayette, CO). Each pool consisted of four oligonucleotides targeting a different region of the same gene. Each assay plate included the following controls: nontargeting siRNA, Vps34 and PLK1 (transfection efficiency control) siRNA. siRNAs were transiently transfected in hexplicate into H4 cells stably expressing LC3-GFP reporter at 40 nM final concentration using reverse transfection. HiPerfect reagent (QIAGEN) was diluted 1:20 in DMEM and 8 μL/well of the mixture was aliquoted into 384-well plates using WellMate liquid handling unit (Matrix). Two microliters of 1 μM-arrayed siRNA pools/well were added robotically using Velocity11 Bravo. After 30 min incubation, 500 cells/well in 40 uL full media were added using WellMate. Seventy-two hours post-transfection, the cells were treated with DMSO, rapamycin (200 nM), or rapamycin (200 nM) and spautin (10 μM) for an additional 8 hr, then counterstained with 0.5 μM Hoechst 33342 (Invitrogen) for 1 hr, and fixed with 30 μl of 3.8% paraformaldehyde for 30 min. The cells were washed three times with PBS. The secondary screen used a deconvolved DUB library in which the four components of each siRNA pool were separated into individual wells. The cells were transfected and treated as in primary screen except that siRNAs were used at 30 nM final concentration and HiPerfect was diluted 1:30 in OptiMEM (Invitrogen). The secondary screen was done in triplicate. For follow-up assays, cells were transfected in 96-, 24-, or 6-well plates using reverse transfection with 1–6 μl HiPerfect/mL, 10–30 nM final siRNA concentration, and cells at 5×10^4 to 2×10^5 cells/ml depending on the cell type. Cells were harvested 48–72 hr after transfection.

The cells were imaged using an automated CellWoRx microscope (Applied Precision) at 10 × magnification and 350 nm (Hoechst) and 488 nm (LC3-GFP) wavelengths. The images were quantified using VHSscan and VHSview image analysis software (Cellomics). Total cell number, total LC3-GFP intensity/cell as well as number, area, and intensity of LC3-GFP positive autophagosomes/cell were scored. Dead and mitotic cells were excluded from analysis based on nuclear intensity. The final autophagy score for every well was obtained by multiplying total autophagosome intensity/cell times number of autophagosomes/cell and dividing by average cells intensity. This formula was empirically determined to most accurately measure LC3-GFP translocation from cytosol into autophagosomes as reflected by consistently significant *Z*-scores and p values when using siRNAs against Vps34 controls under assay conditions and to give the highest *Z′*-score (0.34, where $Z' = 1 - (3SD_{rapamycin} + 3SD_{vps34})/(Ave_{rapamycin} - Ave_{vps34})$ (Zhang et al., 1999). Twenty-one preliminary hits were cherry-picked that when knockdown led to decreases in LC3-GFP positive autophagosome puncta compared to that of the levels in the presence of rapamycin by at least 1.5 standard deviation from the plate median. To confirm the roles of these DUBs in mediating autophagy, we analyzed the effects of knocking down these DUBs on the endogenous LC3II and Beclin1 using 3 additional siRNAs for each DUB in both H4 and Bcap-37 cells. The effect of knockdown was confirmed individually by RT-PCR.

The Sequences of siRNA Oligos Used: 5′ to 3′

Atg14L
siRNA-a:
CCGGGAGAGGUUUAUCGACAAGATT
UCUUGUCGAUAAACCUCUCCCGGTT
siRNA-b:
AUCUUCGACGAUCCCAUAUAUUATT
UAAUAUAUGGGAUCGUCGAAGAUTT
siRNA-c:
UACCCUCAGGAAUCUAAUGUACCTT
GGUACAUUAGAUUCCUGAGGGUATT
Beclin1
siRNA-a:
GAGGAGCCAUUUAUUGAAACUCCTT
GGAGUUUCAAUAAAUGGCUCCUCTT
siRNA-b:
CCGUGGAAUGGAAUGAGAUUAAUTT
AUUAAUCUCAUUCCAUUCCACGGTT
siRNA-c:
GAGCUGCCGUUAUACUGUUCUGGTT
CCAGAACAGUAUAACGGCAGCUCTT
p150
siRNA-a:
CCCGUCCAUUCUUGAAUAATT
UUAUUCAAGAAUGGACGGGTT
siRNA-b:
GGACCAAGCACACAAAUCUTT
AGAUUUGUGUGCUUGGUCCTT
siRNA-c:
CCCUGAACAAGUGCUAAAUTT
AUUUAGCACUUGUUCAGGGTT
USP10
siRNA-a:
CCCUGAUGGUAUCACUAAAGA
UUUAGUGAUACCAUCAGGGGT
siRNA-b:
GCUUUGGAUGGAAGUUCUAAT
UAGAACUUCCAUCCAAAGCGA
siRNA-c:
CGACAAGCUCUUGGAGAUAAA
UAUCUCCAAGAGCUUGUCGGG
USP13
siRNA-a:
GCGACAGGGUCUACAAGAACG

UUCUUGUAGACCCUGUCGCCG
siRNA-b:
CGACGAUUAUGAAUAUGAAGA
UUCAUAUUCAUAAUCGUCGCT
siRNA-c:
CUACGAGCAACGAAUAAUAAC
UAUUAUUCGUUGCUCGUAGTG
UVRAG
siRNA-a:
GCCCGGAACAUUGUUAAUATT
UAUUAACAAUGUUCCGGGCTT
siRNA-b:
GUGCUCCAUUUGAACAUAATT
UUAUGUUCAAAUGGAGCACTT
siRNA-c:
CCCUCAGAUAUCCUAUAAUTT
AUUAUAGGAUAUCUGAGGGTT
Vps34
siRNA-a:
AUGGCUGAAACUACCAGUAAAAUTT
AUUUUACUGGUAGUUUCAGCCAUTT
siRNA-b:
UGGCUGGAUAGAUUGACAUUUAGTT
CUAAAUGUCAAUCUAUCCAGCCATT
siRNA-c:
CUGGCUGCACAACAGACAUUUGUTT
ACAAAUGUCUGUUGUGCAGCCAGTT
No target siRNA:
UUCUCCGAACGUGUCACGUTT
ACGUGACACGUUCGGAGAATT

RT-PCR

Total RNA was prepared using RNeasy mini kit (QIAGEN). RNA (1.25 mg) was used for cDNA synthesis using SuperScript First-Strand Synthesis System for RT-PCR (Invitrogen) with oligo dT primers.

In Vitro Class III PI3 kinase Assay

293T cells were transfected with HA-Vps34/GFP-Beclin1. Immunopurified Vps34 complexes using anti-HA were incubated with PtdIns in the presence of γ-^{32}P-ATP. The phosphorylation product was analyzed by thin layer chromatography and followed by autoradiography.

Coimmunoprecipitation

Cells were lysed with RIPA buffer (40mM Tris-HCl, pH 7.5, 150mM NaCl, 0.5% Nonidet P-40, protease inhibitors cocktail (Sigma), 5% glycerol, 10mM NaF). Whole cell lysates obtained by centrifugation were incubated with 5 μg of antibody and protein A or protein G sepharose beads (Invitrogen) overnight at 4C. The immunocomplexes were then washed with RIPA buffer for three times and separated by 12% SDS–PAGE for further western blotting assay.

Cytoplasmic and Nuclear Proteins Fractionation

H4-LC3 Cells were treated with or without spautin-1 (10 μM) for 12 hr, about 10^7 cells were washed with PBS in 4C, and incubated with Buffer A (HEPES (pH = 7.9), 20 mM; KCl, 10 mM; EDTA, 1 mM; PMSF, 0.5 mM; 1x protease inhibitor cocktail; DTT, 1 mM; NaF, 5 mM; Na_3VO_4, 0.1 mM; Glycerol,10%) at 4C for 10 min. The cell lysates were collected into cold 1.5 ml EP tube and NP-40 was added to the final concentration of 0.5%. After a brief vortexing and incubation in ice (1 min), the lysates were centrifuged at 12500 rpm for 3 min. The supernatant was collected as the cytoplasmic fraction. 50 μl Buffer B (HEPES (pH = 7.9), 20 mM; KCl, 10 mM; EDTA, 1 mM; PMSF, 0.5 mM; 1x protease inhibitor cocktail; DTT, 1 mM; NaF, 5 mM; Na_3VO_4, 0.1 mM; NaCl, 420 mM; Glycerol, 10%) was added into to the sediment. The mixture was vortexed and incubated on ice for 40 min before centrifuged at 12500 rpm for 3 min. The supernatant was collected as the nuclear fraction.

Ub-AMC Assay

Expressed proteins were purified from 293T cells individually transfected with relevant expression constructs by immunoprecipitation followed by extensive washing (12x) and elution with tag peptides. To initiate the enzyme reaction, indicated proteins plus Ub-AMC mixture were added to each well, samples were then incubated for 45 min. Ub–AMC hydrolysis was measured at Ex355/Em460 using an Envision plate reader (Thermo). The final concentrations of every protein and Ub–AMC were about 20 nM and 0.8 μM respectively. Enzymes and substrates were mixed in Ub–AMC assay buffer (50mM Tris-HCl (pH 7.5), 1mM EDTA, 1mM ATP, 5 mM MgCl2, 1mM DTT, and 1 mg/ml ovalbumin). To obtain the IC_{50} of spautin-1, different concentrations of spautin-1 (20 μM to 100 nM) were added and incubated for 30 min. Ub-AMC was then added to each well and incubated for another 45 min. Ub–AMC hydrolysis was measured at Ex355/Em460 using an Envision plate reader (Thermo). % of inhibition was determined and the curve fitting was performed using GraphPad Prism 4.

Electron Microscopy

Pretreated cells were fixed in 2.5% glutaraldehyde, dehydrated and embedded. Ultrathin sections (90 nm) were cut, stained and analyzed by a JEM 1230 electron microscope (JEOL).

SUPPLEMENTAL REFERENCES

Dowler, S., Kular, G., and Alessi, D.R. (2002). Protein lipid overlay assay. Sci. STKE *2002*, pl6.

Gozani, O., Karuman, P., Jones, D.R., Ivanov, D., Cha, J., Lugovskoy, A.A., Baird, C.L., Zhu, H., Field, S.J., Lessnick, S.L., et al. (2003). The PHD finger of the chromatin-associated protein ING2 functions as a nuclear phosphoinositide receptor. Cell *114*, 99–111.

Yuan, J., Luo, K., Zhang, L., Cheville, J.C., and Lou, Z. (2010). USP10 regulates p53 localization and stability by deubiquitinating p53. Cell *140*, 384–396.

Zhang, J.H., Chung, T.D., and Oldenburg, K.R. (1999). A Simple Statistical Parameter for Use in Evaluation and Validation of High Throughput Screening Assays. J. Biomol. Screen. *4*, 67–73.

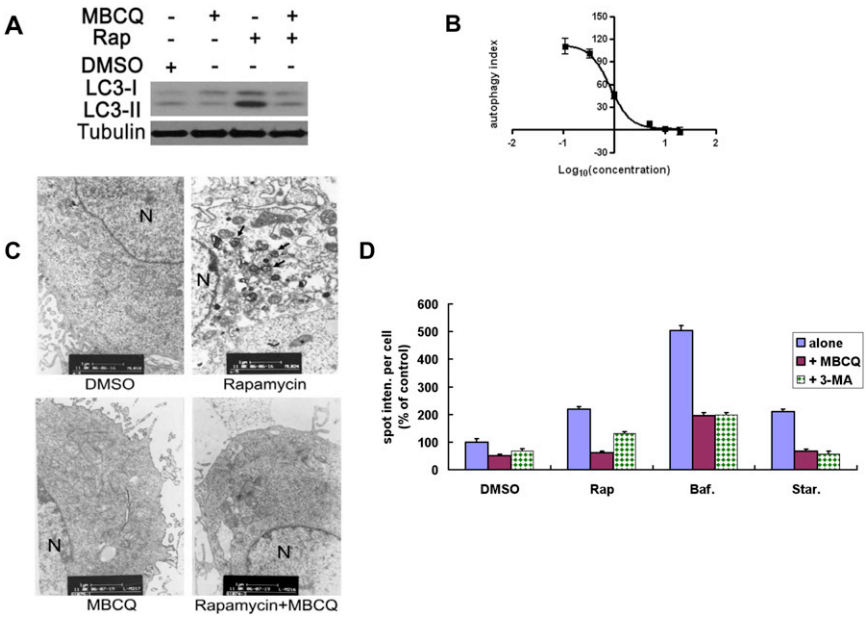

Figure S1. MBCQ Inhibits Autophagy, Related to Figure 1

(A) MEF cells were treated with rapamycin (0.2 μM) in the presence or absence of MBCQ (10 μM) and the cell lysates were analyzed by western blotting using anti-LC3. β-tubulin was used as a control. Rap, rapamycin.

(B) Dose-response curve (in μM) of MBCQ mediated autophagy inhibition in H4-LC3-GFP cells treated with rapamycin (0.2 μM) for 12 hr. The LC3-GFP$^+$ puncta were quantified as in Figure 1F. Autophagy index = % {[total LC3-GFP$^+$ spot intensity (compound+rapamycin treated) per cell] – [total LC3-GFP$^+$ spot intensity (DMSO treated) per cell]} / {[total LC3-GFP$^+$ spot intensity (rapamycin treated) per cell] – [total LC3-GFP$^+$ spot intensity (DMSO treated) per cell]}.

(C) H4-LC3-GFP cells were treated with vehicle control (1‰ DMSO), rapamycin (0.2 μM) alone or in the presence of MBCQ (10 μM) for 4 hr. The cells were then fixed with glutaraldehyde and prepared for EM analysis. Bar, 1:11,000. Arrows indicate double and multimembrane autophagosomic vesicles. N, nucleus.

(D) H4-LC3-GFP cells were treated as indicated for 4 hr. Baf, Bafilomycin A1 (80 nM); Rap, rapamycin (0.2 μM); 3-MA (10 mM); MBCQ (10 μM); Star, starvation in Hanks buffer. The cells were fixed with 4% paraformaldehyde and the levels of GFP-LC3 spot intensity per cell were measured using ArrayScan HCS. All error bars indicate STD.

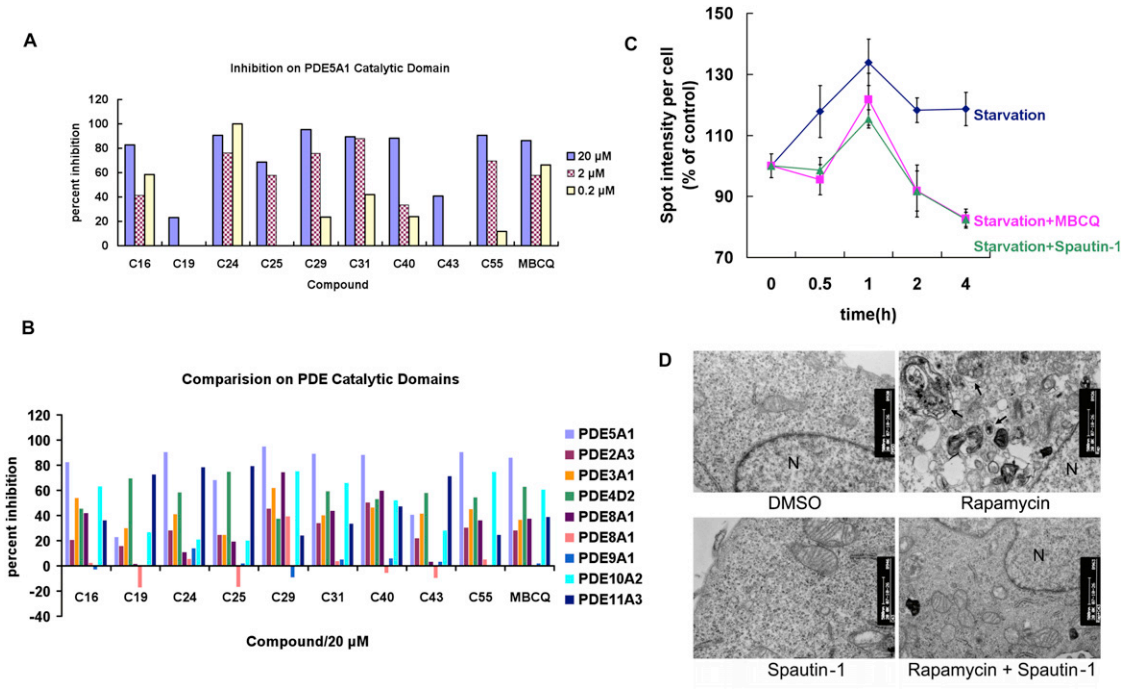

Figure S2. Separation of PDE Inhibiting Activity and Autophagy Inhibiting Activity in MBCQ by Medicinal Chemistry, Related to Figure 1

Recombinant PDE5 (A) or other PDEs (B) were incubated with indicated MBCQ derivatives in a reaction mixture containing 20 mM Tris HCl, pH 7.5, 10 mM $MgCl_2$, ^{3}H-cGMP or ^{3}H-cAMP at 25C for 15 min. The reaction was terminated by the addition of 0.2 M $ZnSO_4$ and 0.125 M $Ba(OH)_2$. The reaction product ^{3}H-GMP or ^{3}H-AMP was precipitated by $BaSO_4$ while un-reacted ^{3}H-cGMP or ^{3}H-cAMP remained in the supernatant. Radioactivity in the supernatant was measured by liquid scintillation counting. (C) H4-LC3 cells were treated with MBCQ (10 μM) or spautin-1 (10 μM) for indicated time in Hanks buffer without glucose. The cells were fixed and stained with DAPI. The levels of LC3-GFP spot intensity per cell were measured using ArrayScan HCS. (D) MEF cells were treated with vehicle control (1‰ DMSO), and spautin-1 (10 μM) as indicated for 4 hr. The cells were then fixed with glutaraldehyde and prepared for EM analysis. Bar, 1:11,000. Arrows indicate double and multimembrane autophagosomic vesicles. N, nucleus. All error bars indicate STD.

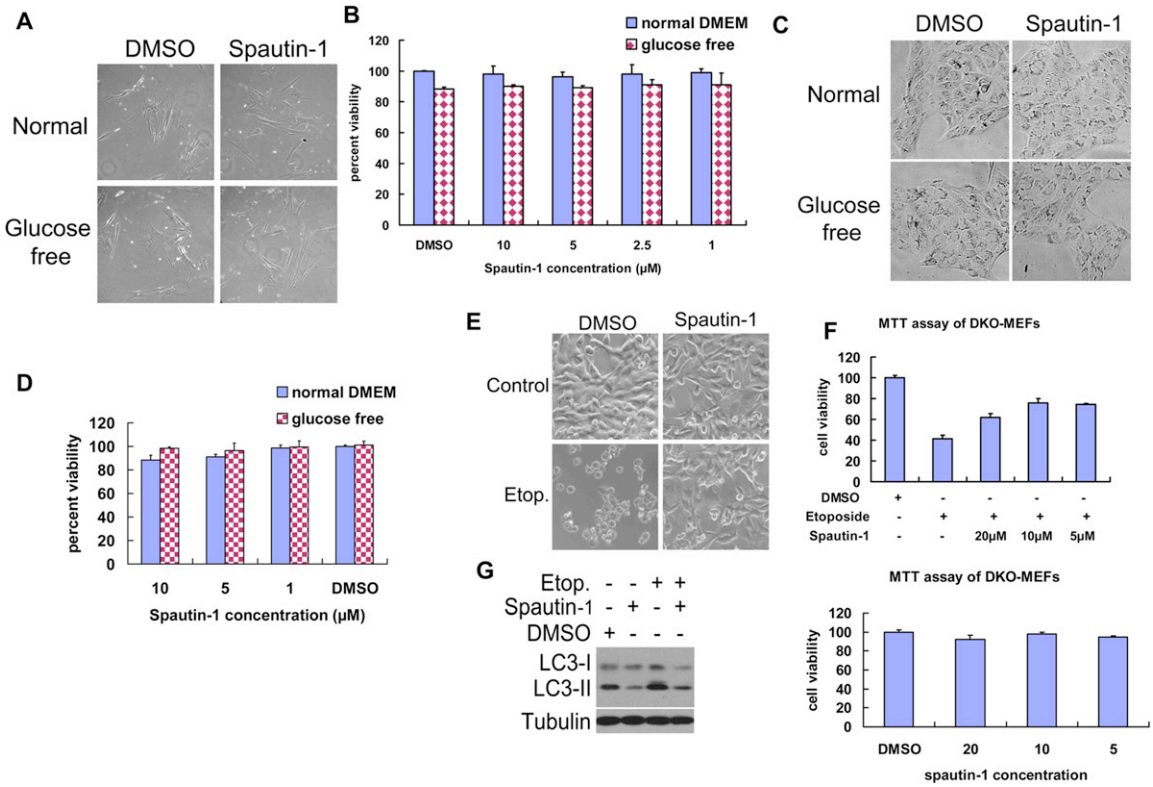

Figure S3. Inhibition of Autophagy by Spautin-1 Effects Cell Death and Cell Survival, related to Figure 2

(A and B) MDCK cells were treated with DMSO (1‰) and spautin-1 (10 μM) in normal or glucose-free conditions for 24 hr. The images were recorded with a phase contrast microscope (A). The cell survival was analyzed by MTT assay (B).

(C) and (D) Hs578Bst cells were treated with DMSO (1‰) and spautin-1 (10 μM) in DMEM with or without glucose for 24 hr. The images were recorded using a phase contrast microscope (C) or MTT assay (D).

(E-G) Bax/Bak DKO cells were treated with spautin-1 (10 μM), in the presence or absence of etoposide (8 μM) for 8 hr. The images were recorded with a phase contrast microscope (E). Cell survival was determined by MTT assay (F). The cell lysates were analyzed by western blotting using anti-LC3 antibody with anti-β-tubulin as a control (G). Etop, etoposide.

All error bars indicate STD.

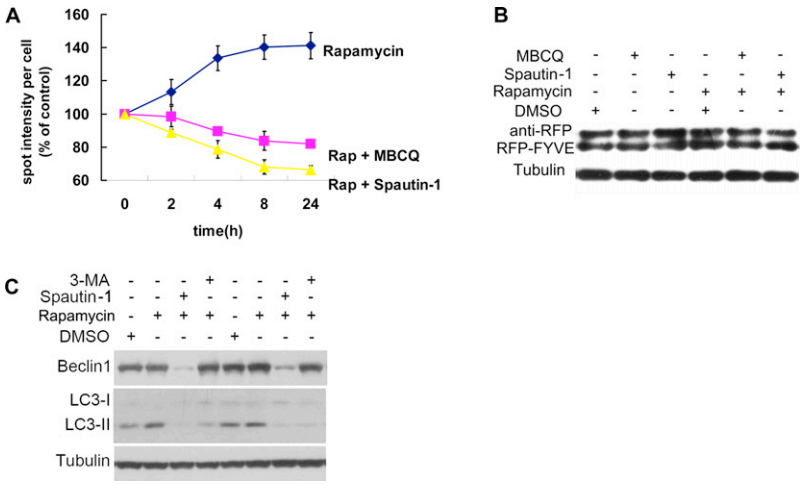

Figure S4. Spautin-1 Reduces the Levels of PtdIns3P, Related to Figure 3

(A) H4-FYVE-RFP cells were treated with rapamycin (0.2 μM) in the presence or absence of MBCQ (10 μM) or spautin-1 (10 μM) as indicated. The cells were fixed with 4% paraformaldehyde and imaged using ArrayScan HCS 4.0 Reader with a 20X objective. The data are expressed as % of control vehicle treated cells. 1000 cells were analyzed for per treatment condition. Rap, rapamycin.

(B) The cell lysates were collected after 8 hr treatment with indicated compounds and analyzed by western blotting using anti-RFP and anti-β-tubulin.

(C) H4 cells were treated with rapamycin (0.2 μM), spautin-1 (10 μM) or 3-MA (10 mM) alone or in combination as indicated for 4 hr, and DMSO (1‰) was used as negative control. The cell lysates were analyzed by western blotting using anti-Beclin1 and anti-LC3. Anti-β-tubulin was used as loading controls.

All error bars indicate STD.

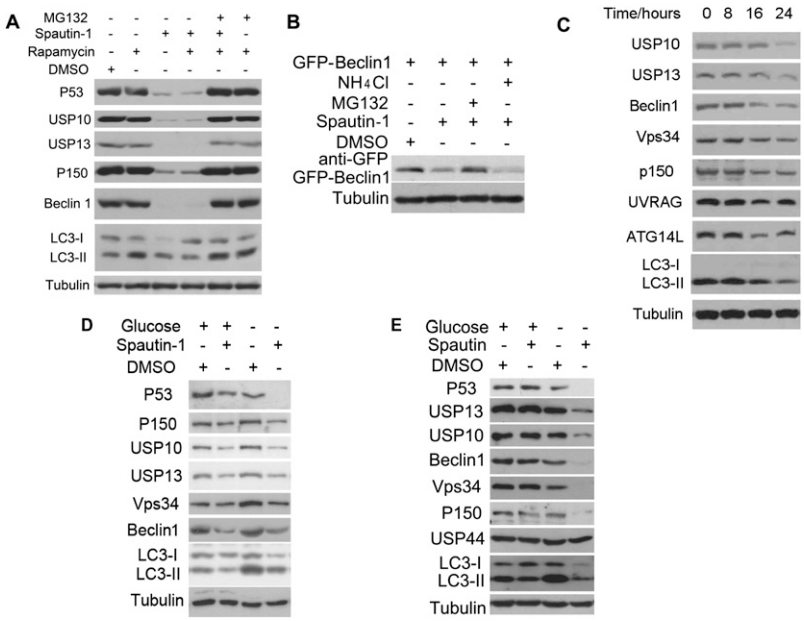

Figure S5. Spautin-1 Promotes the Degradation of Beclin1 via the Proteasome Pathway, Related to Figure 4

(A) H4-LC3-GFP cells were treated with rapamycin (0.2 μM), spautin-1 (10 μM) and MG132 (25 μM) for 6 hr. The cell lysates were analyzed by western blotting using indicated antibody.

(B) 293T cells were transfected with GFP-Beclin1 and 24 hr after the transfection, the cells were treated with indicated compounds for an additional 4 hr. DMSO (1‰), MBCQ (10 μM), spautin-1 (10 μM), NH_4Cl (10 mM), MG132 (10 μM). The cell lysates were analyzed by western blotting using anti-GFP.

(C) MEF cells were treated with spautin-1 (10 μM) for indicated periods of time, the cell lysates were analyzed by western blotting using indicated antibodies. β-tubulin was used as a control.

(D) HeLa cells were treated with spautin-1 (10 μM) in normal DMEM or glucose free DMEM for 8 hr, the cell lysates were analyzed by western blotting with indicated antibodies. β-tubulin was used as a control.

(E) Bcap-37 cells were treated with spautin-1 (10 μM) in normal DMEM or glucose free DMEM for 12 hr, the cell lysates were analyzed by western blotting with indicated antibodies. β-tubulin was used as a control.

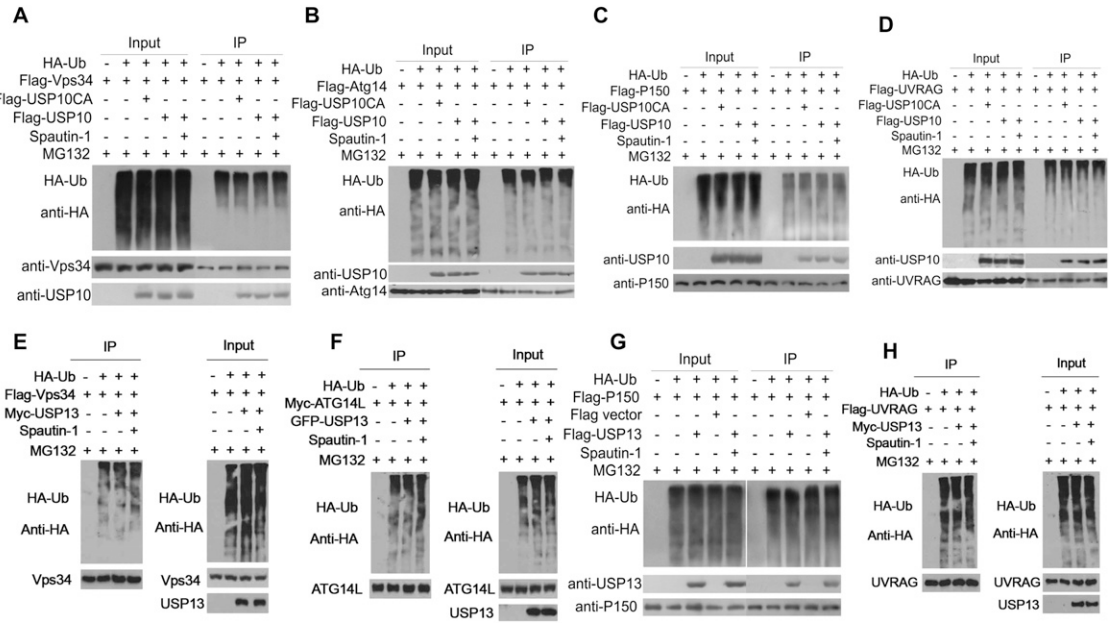

Figure S6. Targeting Specificity of USP10 and USP13, Related to Figure 5

(A-D) Overexpression of USP10 has no obvious effect on the ubiquitination levels of Vps34 (A), Atg14L (B), p150 (C) and UVRAG (D). 293T cells were transfected with indicated expression vectors for 12 hr, incubated with MG132 (10 μM) in the presence or absence of spautin-1 (10 μM) for an additional 4 hr. The cell lysates were immunoprecipitated with antibodies for indicated proteins ([(A)] anti-Vps34 for flag-Vps34; [(B)] anti-myc for myc-Atg14L; [(C)] anti-p150 for flag-p150; [(D)] anti-UVRAG for flag-UVRAG) and the immunocomplexes were analyzed by western blotting using anti-HA antibody.

(E-H) Overexpression of USP13 has no obvious effects on the ubiquitination levels of (E), Atg14L (F), p150 (G) and UVRAG (H). 293T cells were transfected with indicated expression vectors for 12 hr, incubated with MG132 (10 μM) in the presence or absence of spautin-1 (10 μM) for an additional 4 hr. The cell lysates were immunoprecipitated with indicated antibodies ([(E)] anti-Vps34 for flag-Vps34; [(F)] anti-Atg14L for myc-Atg14L; [(G)] anti-p150 for flag-p150; [(H)] anti-UVRAG for flag-UVRAG) and the immunocomplexes were analyzed by western blotting using anti-HA antibody.

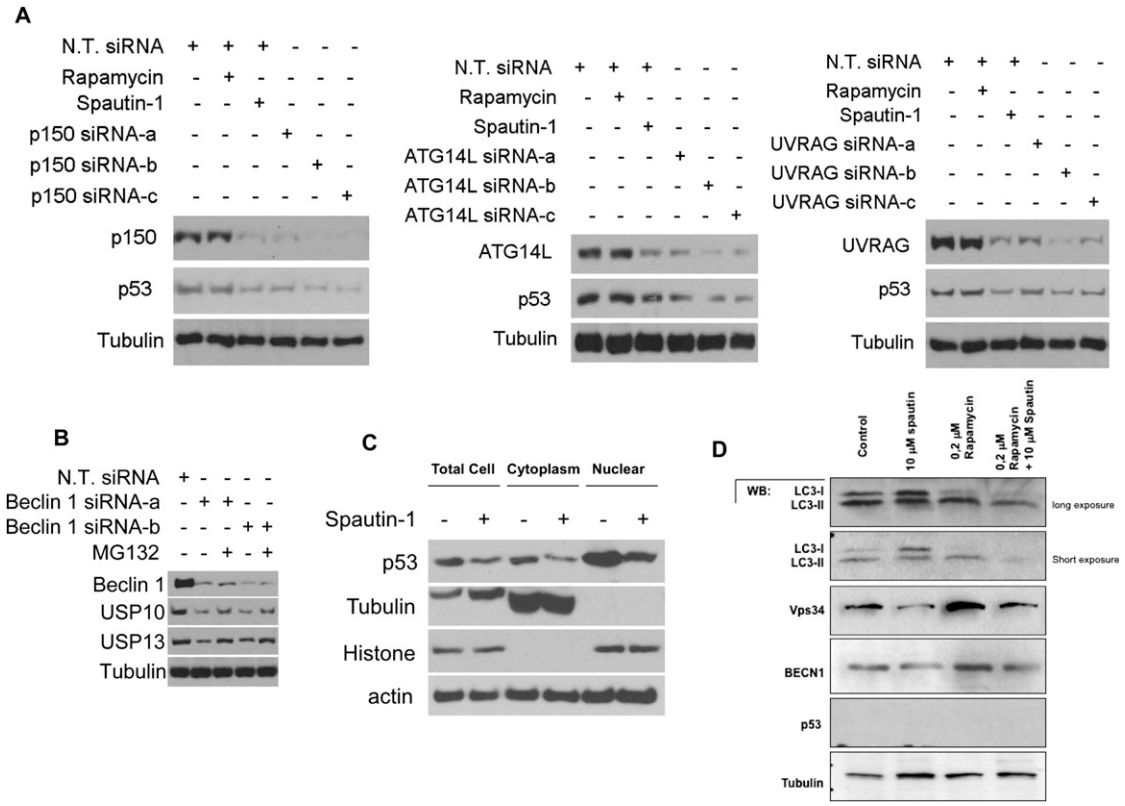

Figure S7. Spautin-1 Promotes the Degradation of p53, which Is Regulated by Vps34 Complexes, Related to Figure 6

(A) H4-LC3-GFP cells were transfected with indicated siRNAs for 72 hr or treated with rapamycin (0.25 μM) or spautin-1 (10 μM) for 4 hr, the cell lysates were analyzed by western blotting using indicated antibodies. β-tubulin was used as a control.

(B) H4-LC3-GFP cells were transfected with indicated siRNAs for 64 hr and treated with or without MG132 (10 μM) for plus 8 hr, the cell lysates were analyzed by western blotting using indicated antibodies. β-tubulin was used as a control.

(C) H4-LC3-GFP Cells were treated with or without spautin-1 (10 μM) for 12 hr, cytoplasmic and nuclear fractions were fractionated and analyzed by western blotting using anti-p53 antibody. Anti-β-tubulin (for cytoplasmic fraction), anti-actin and anti-histone (for nuclear fraction) were used as controls.

(D) The effect of spautin-1 on p53 null ovarian cancer cells. SKOV-3 cells were treated with spautin-1 (10 μM) or rapamycin (0.2 μM) alone, or in combination in normal RPMI medium supplemented with 10% bovine serum for 24 hr. DMSO (1‰) was used as a negative control. The cell lysates were analyzed by western blotting using anti-LC3, anti-Vps34, anti-Beclin1, anti-USP10, anti-USP13, anti-p53 and anti-b-tubulin (as a control).